Chemistry of Dimetallaboranes Derived from the Reaction of $[Cp^*MCl_2]_2$ with Monoboranes (M = Ru, Rh; $Cp^* = \eta^5$-C_5Me_5)

Xinjian Lei, Maoyu Shang, and Thomas P. Fehlner*

Contribution from the Department of Chemistry and Biochemistry, University of Notre Dame, Notre Dame, Indiana 46556-5670

Received August 17, 1998

Abstract: In a single step, from $[Cp^*RuCl_2]_2$ ($Cp^* = \eta^5$-C_5Me_5) and $Li[BH_4]$, *nido*-1,2-$(Cp^*Ru)_2(\mu$-$H)_2B_3H_7$, **1**, is produced in high yield. Addition of BH_3·THF to **1** results in conversion to *nido*-1,2-$(Cp^*Ru)_2(\mu$-$H)B_4H_9$, **2**. Reaction of BH_3·THF directly with $[Cp^*RuCl_2]_2$ yields a mixture of **1** and **2**. In two steps, a rhodium analogue, *nido*-2,3-$(Cp^*Rh)_2B_3H_7$, **9**, is accessible by the reaction of $[Cp^*RhCl_2]_2$ and $Li[BH_4]$ to exclusively produce $(Cp^*Rh)_2B_2H_6$, **8**, which adds BH_3·THF to give **9** as the major product in a mixture. Reaction of BH_3·THF directly with $[Cp^*RhCl_2]_2$ yields the chloro derivative of **9**, *nido*-1-Cl-2,3-$(Cp^*Rh)_2B_3H_6$, **11**, in high yield via the intermediate positional isomer, *nido*-3-Cl-1,2-$(Cp^*Rh)_2B_3H_6$, **10**. With high concentrations of $Co_2(CO)_8$, **1** reacts with $Co_2(CO)_8$ to give *nido*-1-(Cp*Ru)-2-(Cp*RuCO)-3-$Co(CO)_2(\mu_3$-$CO)B_3H_6$, **3**, whereas low concentrations permit competitive degradation of **1** to yield *arachno*-(Cp*Ru)$(CO)(\mu$-$H)B_3H_7$, **4**. On the other hand, reaction of **11** with $Co_2(CO)_8$ gives *closo*-1-Cl-6-$\{Co(CO)_2\}$-2,3-$(Cp^*Rh)_2(\mu_3$-$CO)B_3H_3$, **12**. Mild thermolysis of **3** results in loss of hydrogen and the formation of *closo*-6-$Co(CO)_2$-2,3-$(Cp^*Ru)_2(\mu$-$CO)(\mu_3$-$CO)B_3H_4$, **5**, whereas thermolysis of **2** results in loss of hydrogen and formation of *pileo*-2,3-$(Cp^*Ru)_2B_4H_8$, **6**, with a BH-capped square pyramidal structure. Finally, **6** reacts with $Fe_2(CO)_9$ to yield *pileo*-6-$Fe(CO)_3$-2,3-$(Cp^*Ru)_2(\mu_3$-$CO)B_4H_4$, **7**, with a BH-capped octahedral cluster structure. The overall isolated yield of **7**, formed in four steps from $[Cp^*RuCl_2]_2$, is ≈50% and evidences good control of reactivity.

Introduction

Metallaborane chemistry echoes organometallic chemistry in that borane and transition metal fragments are mutually stabilized through their bonding interactions.[1] Just as with the hydrocarbon and transition metal fragments of an organometallic compound,[2] the mutual perturbation of electronic structure and properties promotes (or inhibits) reactions of the borane fragment and, likewise, the metal fragment. At the level of electron-counting rules,[3,4] the principles governing geometric structure of metallaboranes are verified in numerous examples[5−9] and our level of understanding approaches that of structural organometallic chemistry. The same cannot be said for synthetic metallaborane chemistry in that the proven methods for the formation of compounds containing metal−boron bonds are more limited than those for metal−carbon bonds.[7,10] Hence, much of the richness metal variability adds to organometallic chemistry is still lacking in metallaborane chemistry.

Previous synthetic approaches have emphasized the reactions of polyboranes, often anionic, with metal fragment precursors, and these have been particularly successful for monometallic compounds.[11−17] There are two deficiencies in this approach: activated polyboranes are required and polymetallic species are difficult to make selectively. The former requires the synthesis or acquisition of the appropriate polyborane, and the low yields and time-consuming separations associated with the latter stymie the development of derivative chemistry. Both inhibit consideration of potential applications.

In recent years we have been exploring the reactions of monocyclopentadienylmetal chloride dimers with commercially available monoboranes as a general route to dimetallaboranes. Full descriptions of the Co,[18] Cr,[19] and Mo[20] systems have been reported to date. The metal dimer serves as a scaffold upon which a polyborane fragment assembles under mild conditions. Under kinetic control, the monoborane activates the metal dimer by removing Cl (as Cl^- for $[BH_4]^-$ or, with the exception of Cr, BH_2Cl for BH_3·THF) and high yields of single compounds are observed. Thus, in a single step both M−B and B−B bonds are formed with high selectivity. Others have used monoboranes

(1) *Inorganometallic Chemistry*; Fehlner, T. P., Ed.; Plenum: New York, 1992.
(2) Elschenbroich, C.; Salzer, A. *Organometallics*; VCH: New York, 1989.
(3) Wade, K. *Adv. Inorg. Chem. Radiochem.* **1976**, *18*, 1.
(4) Mingos, D. M. P.; Wales, D. J. *Introduction to Cluster Chemistry*; Prentice Hall: New York, 1990.
(5) Kennedy, J. D. *Prog. Inorg. Chem.* **1984**, *32*, 519.
(6) Kennedy, J. D. *Prog. Inorg. Chem.* **1986**, *34*, 211.
(7) Housecroft, C. E. *Boranes and Metalloboranes*; Ellis Horwood: Chichester, U.K., 1990.
(8) Housecroft, C. E. *Adv. Organomet. Chem.* **1991**, *33*, 1.
(9) Housecroft, C. E. *Cluster Molecules of the p-Block Elements*; Oxford University Press: Oxford, U.K., 1994.
(10) Woollins, J. D. *Non-Metal Rings, Cages and Clusters*; Wiley: New York, 1988.
(11) Greenwood, N. N.; Ward, I. M. *Chem. Soc. Rev.* **1974**, *3*, 231.
(12) Wegner, P. A. In *Boron Hydride Chemistry*; Muetterties, E. L., Ed.; Academic Press: New York, 1975; p 431.
(13) Shore, S. G. *Pure Appl. Chem.* **1977**, *49*, 717.
(14) Grimes, R. N. *Acc. Chem. Res.* **1978**, *11*, 420.
(15) Gaines, D. F. In *Boron Chemistry-4*; Parry, R. W., Kodama, G., Eds.; Pergamon: Oxford, U.K., 1980; p 73.
(16) Housecroft, C. E.; Fehlner, T. P. *Adv. Organomet. Chem.* **1982**, *21*, 57.
(17) Grimes, R. N. In *Metal Interactions with Boron Clusters*; Grimes, R. N., Ed.; Plenum: New York, 1982; p 269.
(18) Nishihara, Y.; Deck, K. J.; Shang, M.; Fehlner, T. P.; Haggerty, B. S.; Rheingold, A. L. *Organometallics* **1994**, *13*, 4510.
(19) Ho, J.; Deck, K. J.; Nishihara, Y.; Shang, M.; Fehlner, T. P. *J. Am. Chem. Soc.* **1995**, *117*, 10292.
(20) Aldridge, S.; Shang, M.; Fehlner, T. P. *J. Am. Chem. Soc.* **1998**, *120*, 2586.

10.1021/ja982954j CCC: $18.00
Published on Web 01/27/1999

to good effect in the formation of metallaboranes. Particularly noteworthy are the dimetallaboranes of Ta[21] and Nb,[22] the metallaborane analogues of mononuclear ethylene complexes,[23−27] the formation of a chloroborohydride complex,[28] the chemistry of a triosmaborane,[29−32] and the metallaborane chemistry associated with certain Mo- and W-based organometallic compounds.[27,33−35]

Herein we describe the application of our approach to dimetal ruthena- and rhodaboranes.[36] A large number of metallaboranes containing one or more group 8 $M(CO)_3$ fragments have been characterized,[5−7,37]but there are few crystallographically characterized examples containing simple group 8 CpM fragments, Cp = η^5-C_5R_5.[24,33,38−41] Likewise, a number of mononuclear rhodaboranes are known,[42,43] but dinuclear rhodaboranes are virtually unstudied.[44]

The present work was initiated with three questions in mind. The first concerned synthesis. Would a route based on the reactions of monoboranes with monocyclopentadienylmetal chorides provide useful syntheses of metallaboranes containing diruthenium and dirhodium fragments? The second involved structure. Fragments such as $M(CO)_3$ (M = Fe, Ru, Os, CpM; M = Co, Rh) which are three-orbital, two-electron species, readily participate in cluster bonding.[14,45] As the CpRu fragment has one electron less than the CpRh fragment, what structural features would compensate in related dimetallaboranes containing the two metals? The third, and most important one, concerned reactivity. Given the characteristic compositional and structural features of the Rh and Ru metallaboranes, what similarities and differences in reactivity would result? Clear answers to these questions would serve to forge another connection between metallaborane chemistry and organometallic chemistry.

Experimental Section

Syntheses. (a) General Information. All operations were conducted under argon atmosphere using standard Schlenk techniques. Solvents were distilled before use under N_2 as follows: sodium benzophenone ketyl for hexane, diethyl ether, and tetrahydrofuran. BH_3·THF (1.0 M in THF), $LiBH_4$(2.0 M in THF), $[Cp^*RhCl_2]_2$, and $Fe_2(CO)_9$ were used as received from Aldrich. Likewise $[Cp^*RuCl_2]_2$ and $Co_2(CO)_8$ (Strem) were used as received. Note that although Cp^*RuCl_2 is described as a polymer in the solid state, it is thought to exist as a dimer in solution.[46] Silica gel (60−200 mesh) was purchased from J. T. Baker Inc. and predried at 140 °C before use. Chromatography was carried out on 3 cm of silica gel in a 2.5 cm diameter column. NMR spectra were recorded on a 300 or 500 MHz Varian FT-NMR spectrometer. Residual protons of solvent were used as reference (δ, ppm, benzene, 7.15) while a sealed tube containing $[(Me_4N)(B_3H_8)]$ in acetone-d_6 (δ_B, ppm, −29.7) was used as the external reference for the ^{11}B NMR. Infrared spectra were obtained on a Nicolet 205 FT-IR spectrometer. Mass spectra (*m*/*z*) were obtained on a JEOL JMS-AX505HA mass spectrometer using the EI ionization mode or the FAB mode in a 3-nitrobenzyl alcohol matrix. Perfluorokersene was used as the standard for the high-resolution EI mass spectra. Elemental analysis was performed by M-H-W Laboratories, Phoenix, AZ.

(b) *nido*-1,2-$(Cp^*Ru)_2(\mu$-H$)_2B_3H_7$, 1. In a typical reaction, $[Cp^*RuCl_2]_2$ (0.40 g, 0.64 mmol) was placed in a 100 mL Schlenk tube with 30 mL of freshly distilled THF to generate a red suspension. The mixture was chilled to −40 °C, and $LiBH_4$ (1.6 mL, 3.2 mmol) was added slowly by syringe. The reaction mixture was allowed to warm slowly to room temperature. The red slurry became a red solution within 10 min, along with release of gas. After 1 h of stirring, the THF was removed under vacuum, and the resulting residue was extracted with hexane. Column chromatography was applied, and elution with hexane gave a yellow band from which 0.27 g of **1** was isolated (82% based on the Ru). MS(FAB): P^+ = 516, 3 B, 2 Ru atoms; calcd for weighted average of isotopomers lying within the instrument resolution, 516.1418; obsd, 516.1404. NMR: ^{11}B (hexane, 22 °C), δ −0.5 (d, J_{B-H} = 120 Hz, {^{1}H}, s, 1B), −2.5 (dd, J_{B-H} = 100, 60 Hz, {^{1}H}, s, 2B); ^{1}H (C_6D_6, 22 °C), 3.28 (partially collapsed quartet, pcq, 1H, B−H_t), 2.66 (pcq, 2H, B−H_t), 1.93 (s, 15H, C_5Me_5), 1.79 (s, 15H, C_5Me_5), −4.05 (s, br, 2H, B−*H*−B), −11.25 (pcq, 2H, B−*H*−Ru), −13.55 (s, 2H, Ru−*H*−Ru). IR (hexane, cm^{-1}): 2498 m, 2450 m, 2426 w (B−H_t). Anal. Calcd for $C_{20}H_{39}B_3Ru_2$: C, 46.73; H, 7.65. Found: C, 46.65; H, 7.79.

(c) *nido*-1,2-$(Cp^*Ru)_2(\mu$-H$)B_4H_9$, 2. Two equivalents of BH_3·THF (0.38 mL, 0.38 mmol) was added to **1** (0.10 g, 0.19 mmol) in 10 mL of THF, and the solution was stirred at 60 °C for 10 h. Filtration and removal of the THF afforded 0.096 g of orange crystals of **2** (95% based on the Ru). MS(FAB): P^+ = 528, 4 B, 2 Ru atoms; calcd for weighted average of isotopomers lying within the instrument resolution, 528.1589; obsd, 528.1602. NMR: ^{11}B (hexane, 22 °C), δ 17.1 (dd, J_{B-H} = 110 Hz, 56 Hz,{^{1}H}, s), 3.9 (d, J_{B-H} = 120 Hz, {^{1}H}, s); ^{1}H (C_6D_6, 22 °C), 3.36 (pcq, 2H, B−H_t), 2.70 (pcq, 2H, B−H_t), 1.85 (s, 15H, C_5Me_5), 1.81 (s, 15H, C_5Me_5), −3.62 (s,br, 1H, B−*H*−B), −3.93 (s, br, 2H, B−*H*−B), −13.39 (br, 2H, B−*H*−Ru), −13.50 (s, 1H, Ru−*H*−Ru). IR (hexane, cm^{-1}): 2500 m, 2434 m. Anal. Calcd for $C_{20}H_{40}B_4Ru_2$: C, 45.68; H, 7.67. Found: C, 45.84; H, 7.44.

(d) *nido*-1-(Cp*Ru)-2-(Cp*RuCO)-3-Co$(CO)_2(\mu_3$-CO$)B_3H_6$, 3. 1 (0.13 g, 0.25 mmol) and $Co_2(CO)_8$ (0.13 g, 0.38 mmol) in 10 mL of hexane were stirred for 15 h at room temperature to give a greenish brown solution. A ^{11}B NMR spectrum of the resulting solution showed a major boron-containing product plus small amounts of other boron-contaning species. Column chromatography with hexane removed a dark brown band ($Co_4(CO)_{12}$) and a bright orange band ($[Cp^*Ru(CO)_2]_2$).[47] Elution with ether then afforded a greenish brown solution

(21) Ting, C.; Messerle, L. *J. Am. Chem. Soc.* **1989**, *111*, 3449.
(22) Brunner, H.; Gehart, G.; Meier, W.; Wachter, J.; Wrackmeyer, B. *J. Organomet. Chem.* **1992**, *436*, 313.
(23) Medford, G.; Shore, S. G. *J. Am. Chem. Soc.* **1978**, *100*, 3953.
(24) Plotkin, J. S.; Shore, S. G. *J. Organomet. Chem.* **1979**, *182*, C15.
(25) Coffy, T. J.; Medford, G.; Plotkin, J.; Long, G. J.; Huffman, J. C.; Shore, S. G. *Organometallics* **1989**, *8*, 2404.
(26) Coffy, T. J.; Shore, S. G. *J. Organomet. Chem.* **1990**, *394*.
(27) Grebenik, P. D.; Leach, J. B.; Green, M. L. H.; Walker, N. M. *J. Organomet. Chem.* **1988**, *345*, C31.
(28) Kawano, Y.; Shimoi, M. *Chem. Lett.* **1998**, 935.
(29) Jan, D.-Y.; Hsu, L.-Y.; Workman, D. P.; Shore, S. G. *Organometallics* **1987**, *6*, 1984.
(30) Krause, J. K.; Jan, D.-Y.; Shore, S. G. *J. Am. Chem. Soc.* **1987**, *109*, 4416.
(31) Jan, D.-Y.; Workman, D. P.; Hsu, L.-Y.; Krause, J. A.; Shore, S. G. *Inorg. Chem.* **1992**, *31*, 5123.
(32) Chung, J.-H.; Boyd, E. P.; Liu, J.; Shore, S. G. *Inorg. Chem.* **1997**, *36*, 4778.
(33) Grebenik, P. D.; Green, M. L. H.; Kelland, M. A.; Leach, J. B.; Mountford, P.; Stringer, G.; Walker, N. M.; Wong, L.-L. *J. Chem. Soc., Chem. Commun.* **1988**, 799.
(34) Grebenik, P. D.; Green, M. L. H.; Kelland, M. A.; Leach, J. B.; Mountford, P. *J. Chem. Soc., Chem. Commun.* **1989**, 1387.
(35) Bullick, H. J.; Grenbenik, P. D.; Green, M. L. H.; Hughes, A. K.; Leach, J. B.; McGowan, P. C. *J. Chem. Soc., Dalton Trans.* **1995**, 67.
(36) Lei, X.; Shang, M.; Fehlner, T. P. *J. Am. Chem. Soc.* **1998**, *120*, 2686.
(37) Housecroft, C. E. In *Inorganometallic Chemistry*; Fehlner, T. P., Ed.; Plenum Press: New York, 1992; p 73.
(38) Grebenik, P. D.; Green, M. L. H.; Kelland, M. A.; Mountford, P.; Leach, J. B. *New J. Chem.* **1992**, *16*, 19.
(39) Suzuki, H.; Takaya, Y.; Tada, K.; Kakigano, T.; Igarashi, M.; Tanaka, M. In *Symposium on Organometallic Chemistry—Abstracts*; Kinki Chemical Society: Tokyo, 1992; p 154.
(40) Weiss, R.; Grimes, R. N. *J. Am. Chem. Soc.* **1977**, *99*, 8087.
(41) Weiss, R.; Grimes, R. N. *Inorg. Chem.* **1979**, *18*, 3291.
(42) Boocock, S. K.; Toft, M. A.; Inkrott, K. E.; Hsu, L.-Y.; Huffman, J. C.; Folting, K.; Shore, S. G. *Inorg. Chem.* **1984**, *23*, 3084.
(43) Fontaine, X. L. R.; Fowkes, H.; Greenwood, N. N.; Kennedy, J. D.; Thornton-Pett, M. *J. Chem. Soc., Dalton Trans.* **1987**, 2417.
(44) Fontaine, X. L. R.; Greenwood, N. N.; Kennedy, J. D.; MacKinnon, P. I.; Thornton-Pett, M. *Chem. Commun.* **1986**, 1111.
(45) Fehlner, T. P. *New J. Chem.* **1988**, *12*, 307.
(46) Kölle, U.; Kossakowski, J. *J. Organomet. Chem.* **1989**, *362*, 383.
(47) King, R. B.; Iqbal, M. Z.; King, A. D. *J. Organomet. Chem.* **1979**, *171*, 53.

which gave 0.10 g of **3** (61% based on Ru). MS(EI): $P^+ = 684$, 3 B, 2 Ru atoms; fragment peaks corresponding to sequential loss of 4 CO; calcd for weighted average of isotopomers lying within the instrument resolution, 684.0312; obsd, 684.0339. NMR: ^{11}B (hexane, 22 °C), δ 65.9 (d, $J_{B-H} = 154$ Hz, {^{1}H}, s, 1B), 20.0 (dd, $J_{B-H} = 60$, 130 Hz, {^{1}H}, s, 1B), 2.0 (d, $J_{B-H} = 150$ Hz, {^{1}H}, s, 1B); ^{1}H (C_6D_6, 22 °C), δ 6.20 (pcq, 1H, B−H_t), 3.80 (pcq, 1H, B−H_t), 2.89 (pcq, 1H, B−H_t), 1.58 (s, 15H, C_5Me_5), 1.50 (s, 15H, C_5Me_5), 0.84 (br, 1H, B−H−M), −2.37 (br, 1H, B−H−B), −4.89 (br, 1H, B−H−M); ^{13}C{^{1}H} (Tol-d_8, 22 °C), δ 212.6 (*C*O), 102.9 (C_5Me$_5$), 102.9 (C_5Me$_5$), 9.6 (C_5Me_5), 9.5 (C_5Me_5). IR (KBr, cm^{-1}): 2511 w, 2443 w (B−H); 2010 vs, 1961 s, 1911 s, 1897 s, sh, 1679 s (CO). Anal. Calcd for $C_{24}H_{36}O_4B_3CoRu_2$: C, 42.26; H, 5.32. Found: C, 42.40; H, 5.67.

(e) *arachno*-(Cp*Ru)(CO)(μ-H)B_3H_7, 4. 1 (0.10 g, 0.19 mmol) and $Co_2(CO)_8$ (0.06 g, 0.18 mmol) were placed in a 100 mL Schlenk tube. A 20 mL portion of freshly distilled hexane was added, and the reaction mixture was stirred for 10 h at room temperature. Column chromatography was performed. Elution with hexane (dark brown solution) followed by ether afforded **3**. The dark brown solution was kept at −40 °C overnight. Black crystals ($Co_4(CO)_{12}$) formed and were removed by filtration. The solution was then concentrated and again kept at −40 °C overnight. The procedure was repeated until the solution IR indicated the absence of $Co_4(CO)_{12}$. The resulting light brown solution was dried to give 0.015 g of **4** (26% based on Ru). MS(EI): $P^+ = 306$, 3 B, 1 Ru atoms; fragment peak corresponding to loss of 1 CO; calcd for weighted average of isotopomers lying within the instrument resolution, 306.1087; obsd, 306.1057. NMR: ^{11}B (hexane, 22 °C), δ 0.8 (d, t, $J_{B-H} = 140$, 40 Hz, {^{1}H}, s, 1B), −2.8 (t, $J_{B-H} = 120$ Hz,{^{1}H}, s, 1B), −11.7 (t, $J_{B-H} = 110$ Hz, {^{1}H}, s, 1B); ^{1}H (C_6D_6, 22 °C), δ 3.18 (pcq, 2H, B−H_t), 2.49 (overlaping pcq, 2H, B−H_t), 2.28 (overlaping pcq, 1H, B−H_t), 1.44 (s, 15H, C_5Me_5), −3.23 (br, 1H, B−H−M), −4.09 (br, 1H, B−H−B), −11.79 (br, 1H, B−H−M). IR (C_6D_6, cm^{-1}): 2521 w, 2482 w, 2435 w, 2422 w (B−H); 1990 vs (CO).

(f) *closo*-6-Co(CO)$_2$-2,3-(Cp*Ru)$_2$(μ-CO)(μ_3-CO)B_3H_4, 5. 3 (0.05 g, 0.07 mmol) was dissolved in 10 mL of freshly distilled toluene. The resulting green brown solution was stirred for 30 min at 80 °C. Column chromatography with hexane gave an orange solution containing [Cp*Ru(CO)$_2$]$_2$. Elution with ether afforded a red-brown solution, which was dried to give 0.03 g of red microcrystals of **5** (66%). Note that longer heating time resulted in decomposition of **5** to [Cp*Ru(CO)$_2$]$_2$. MS (EI): $P^+ = 682$, 3 B, 2 Ru atoms; fragment peaks corresponding to sequential loss of 4 CO; calcd for weighted average of isotopomers lying within the instrument resolution, 682.0192; obsd, 682.0133. NMR: ^{11}B (toluene, 22 °C), δ 82.4 (d, $J_{B-H} = 130$ Hz, {^{1}H}, s, 1B), 49.1 (d, $J_{B-H} = 132$ Hz, {^{1}H}, s, 2B); ^{1}H (C_6D_6, 22 °C), δ 8.50 (pcq, 1H, B−H_t), 6.30 (pcq, 2H, B−H_t), 1.56 (s, 30H, C_5Me_5), −10.25 (br, 1H, Co−H). IR (C_6D_6, cm^{-1}): 2495 w, 2490 w (B−H); 2035 vs, 1991 s, 1825 s, 1755 s (CO).

(g) *pileo*-2,3-{Cp*Ru}$_2$(μ-H)B_4H_7, 6. 2 (0.10 g, 0.19 mmol) was disolved in 5 mL of freshly distilled toluene, and the solution was stirred at 95 °C for 20 h. Filtration and removal of the toluene afforded 0.098 g of orange solid **6** (98%). MS(FAB): $P^+ = 526$, 4 B, 2 Ru atoms; calcd for $^{12}C_{20}{}^1H_{38}{}^{11}B_4{}^{102}Ru_2$, 526.1433; obsd, 526.1432. NMR: ^{11}B (hexane, 22 °C), δ 122.5 (d, $J_{B-H} = 110$ Hz,{^{1}H}, s, 1B), 21.3 (d, $J_{B-H} = 120$ Hz, {^{1}H}, s, 2B), −32.8 (d, $J_{B-H} = 130$ Hz, {^{1}H}, s, 1B); ^{1}H (C_6D_6, 22 °C), 10.01 (pcq, 1H, B−H_t), 5.46 (pcq, 2H, B−H_t), 1.75 (s, 15H, C_5Me_5), −0.27 (s, br, 1H, B−H−B), −2.37 (q, $J_{B-H} = 130$ Hz, 1H, B−H_t), −12.37 (br, 2H, B−H−Ru), −15.08 (s, 1H, Ru−H−Ru). IR (hexane, cm^{-1}): 2492 w, 2528 m. Anal. Calcd for $C_{20}H_{38}B_4Ru_2$: C, 45.85; H, 7.31. Found: C, 46.52; H, 7.25.

(h) *pileo*-6-{Fe(CO)$_3$}-2,3-{Cp*Ru}$_2$-(μ_3-CO)B_4H_4, 7. 6 (0.10 g, 0.19 mmol) and an excess of $Fe_2(CO)_9$ were placed in a 100 mL Schlenk tube. A 10 mL portion of freshly distilled hexane was added to the mixture by syringe. The reaction mixture was stirred for 2 h at 60 °C. Filtration through Celite and column chromatography afforded a red solution, which was dried to give 0.09 g of red microcrystals of **7** (70% based on Ru). MS(EI): $P^+ = 690$, 4 B, 2 Ru atoms; fragment peaks corresponding to sequential loss of 4 CO; calcd for weighted average of isotopomers lying within the instrument resolution, 690.0311; obsd, 690.0293. NMR: ^{11}B (hexane, 22 °C), δ 98.1 (d, $J_{B-H} = 160$ Hz, {^{1}H}, s, 1B), 79.0 (d, $J_{B-H} = 132$ Hz,{^{1}H}, s, 2B), 5.2 (d, $J_{B-H} = 125$ Hz, {^{1}H}, s, 1B); ^{1}H (C_6D_6, 22 °C), δ 8.52 (pcq, 2H, B−H_t), 6.52 (pcq, 1H, B−H_t), 3.11 (pcq, 1H, B−H_t), 1.64 (s, 30H, C_5Me_5). IR (KBr, cm^{-1}): 2576 w, 2474 w, sh, 2454 w (B−H); 2006 vs, 1952 s, 1927 s, 1744 s (CO). IR (hexane, cm^{-1}): 2566 w, 2495 w (B−H); 2020 vs, 1971 s, 1955 s, 1731 s (CO). Anal. Calcd for $C_{24}H_{34}O_4B_4FeRu_2$: C, 41.91; H, 4.98. Found: C, 42.16; H, 5.13.

(i) (Cp*Rh)$_2$$B_2H_6$, 8. [Cp*RhCl$_2$]$_2$ (0.11 g, 0.17 mmol) was placed in a 100 mL Schlenk tube, and 15 mL of freshly distilled THF was added to generate an orange suspension. The mixture was chilled to −40 °C, and $LiBH_4$ (0.43 mL, 0.86 mmol) was added slowly by syringe. The reaction mixture was allowed to warm slowly up to room temperature. The orange slurry became a red-brown solution within 10 min. After 1 h of stirring, the THF was removed under vacuum, and the resulting residue was extracted with hexane. The solution was dried to afford 0.07 g of dark brown **8** (82% based on Rh). MS(EI): $P^+ = 504$, 2 B, 2 Rh atoms; calcd for $^{12}C_{20}{}^1H_{36}{}^{11}B_2{}^{103}Rh_2$, 504.1121; obsd, 504.1119. NMR: ^{11}B (hexane, 22 °C), δ −2.2 (d, $J_{B-H} = 150$ Hz, {^{1}H}, s); ^{1}H (C_6D_6, 22 °C), 9.20 (pcq, 2H, B−H_t), 1.92 (s, 30H, C_5Me_5), −15.64 (s, 4H, B−H−Rh).

(j) *nido*-2,3-{Cp*Rh}$_2$$B_3H_7$, 9. To a solution of **8** (0.08 g, 0.16 mmol) was added 2 equiv of BH_3·THF (0.32 mL, 0.32 mmol) at −40 °C. After the mixture was stirred at room temperature for 1 h and then at 60 °C for 20 h, the solvent was removed under vacuum. Hexane extraction, filtration, and column chromatography at −40 °C afforded a dark red solution. Crystallization at −40 °C gave 0.03 g of dark red crystals of **9** (36%). MS(EI): $P^+ = 516$, 3 B, 2 Rh atoms; calcd for $^{12}C_{20}{}^1H_{37}{}^{11}B_3{}^{103}Rh_2$, 516.1295; obsd, 516.1304. NMR: ^{11}B (hexane, 22 °C), δ 43.9 (d, $J_{B-H} = 150$ Hz, {^{1}H}, 1B), 14.9 (d, $J_{B-H} = 130$ Hz, {^{1}H}, s, 2B); ^{1}H (C_6D_6, 22 °C), δ 5.34 (pcq, 1H, B−H_t), 4.86 (pcq, 2H, B−H_t), 1.83 (s, 30H, C_5Me_5), −2.04 (br, 1H, B−H−B,), −12.09 (br, 2H, Rh−H−B), −16.58 (t, $J_{Rh-H} = 25$ Hz, 1H, Rh−H−Rh). IR (hexane, cm^{-1}): 2497 m, 2455 w (B−H$_t$). Anal. Calcd for $C_{20}H_{37}B_3Rh_2$: C, 46.58; H, 7.23. Found: C, 46.83; H, 7.40.

(k) *nido*-3-Cl-2,3-{η^5-C_5Me_5Rh}$_2$$B_3H_6$, 10. [Cp*RhCl$_2$]$_2$ (0.10 g, 0.16 mmol) was placed in a 100 mL Schlenk tube, and 10 mL of freshly distilled THF was added to generate an orange suspension. The mixture was chilled to −40 °C, and BH_3·THF (1.12 mL, 1.12 mmol) was added slowly by syringe. The reaction mixture was allowed to warm slowly to room temperature. The color of the mixture changed from orange to deep blue and then to red-orange. A homogeneous red-orange solution was observed after a period of 30 min. After the solution was stirred for another 2 h, THF was removed under vacuum, and the resulting residue was extracted with hexane. Low-temperature column chromatography (−20 °C) was applied. Elution with 5% ether in hexane gave a dark red solution, which was dried to afford 0.09 g of **10** (84% based on Rh). MS(EI): $P^+ = 550$, 3 B, 1 Cl, 2 Rh atoms; calcd for $^{12}C_{20}{}^1H_{36}{}^{11}B_3{}^{103}Rh_2{}^{35}Cl$, 550.0907; obsd, 550.0896. NMR: ^{11}B (hexane, 22 °C), δ 48.0 (s, {^{1}H}, 1B), 4.0 (d, $J_{B-H} = 150$ Hz, {^{1}H}, s, 1B), −5.3 (d, $J_{B-H} = 122$ Hz, {^{1}H}, s, 1B); ^{1}H (C_6D_6, 22 °C), δ 3.78 (pcq, 2H, B−H_t), 1.93 (s, 15H, C_5Me_5), 1.73 (s, 15H, C_5Me_5), −4.01 (br, 2H, B−H−B), −14.00 (br, 1H, Rh−H−B,), −14.83 (t, br, $J_{Rh-H} = 25$ Hz, 1H, Rh−H−Rh). IR (hexane, cm^{-1}): 2510 w (B−H$_t$).

(l) *nido*-1-Cl-2,3-{Cp*Rh}$_2$$B_3H_6$, 11. [Cp*RhCl$_2$]$_2$ (0.18 g, 0.28 mmol) was loaded in a 100 mL Schlenk tube, and 20 mL of freshly distilled THF was added to generate an orange suspension. The mixture was chilled to −40 °C, and 1.96 mL (1.96 mmol) of BH_3·THF in THF was added slowly by syringe. The reaction mixture was allowed to warm slowly to room temperature. The color of the mixture changed from orange to deep blue and then to red-orange. A homogeneous red-orange solution was observed over a period of 30 min. The solution was then heated to ca. 65 °C and stirred for 6 h. THF was removed under vacuum, and the resulting residue was extracted with hexane. Column chromatography was applied, and elution with ether gave a red-orange solution, from which 0.14 g of **11** was isolated (91% based on Rh). MS(EI): $P^+ = 550$, 3 B, 1 Cl, 2 Rh atoms; calcd for $^{12}C_{20}{}^1H_{36}{}^{11}B_3{}^{103}Rh_2{}^{35}Cl$, 550.0907; obsd, 550.0896. NMR: ^{11}B (hexane, 22 °C), δ 45.5 (s, {^{1}H}, 1B), 11.5 (d, $J_{B-H} = 120$ Hz, {^{1}H}, s, 2B); ^{1}H (C_6D_6, 22 °C), δ 4.62 (pcq, 2H, B−H_t), 1.74 (s, 30H, C_5Me_5), −2.48 (br, 1H, B−H−B,), −11.63 (br, 2H, Rh−H−B), −15.57 (t, $J_{Rh-H} = 25$ Hz, 1H, Rh−H−Rh). IR (hexane, cm^{-1}): 2510 w (B−H$_t$). Anal. Calcd for $C_{20}H_{36}B_3Rh_2Cl$: C, 43.66; H, 6.60. Found: C, 44.92; H, 6.59.

Table 1. Crystallographic Data and Structure Refinement Details for Compounds **1**, **2**, **3**, and **6**

	1	**2**	**3**	**6**
empirical formula	$C_{20}H_{39}B_3Ru_2$	$C_{20}H_{40}B_4Ru_2$	$C_{24}H_{36}B_3CoO_4Ru_2$	$C_{20}H_{38}B_4Ru_2$
formula weight	514.08	525.90	682.03	523.88
crystal system	monoclinic	tetragonal	monoclinic	triclinic
space group	*C*2/*c*	$I4_1/a$	*Cc*	$P\bar{1}$
a (Å)	11.372(2)	34.003(3)	8.532(3)	8.743(2)
b (Å)	14.061(3)	34.003(3)	38.001(4)	8.901(2)
c (Å)	15.233(3)	8.3206(11)	9.327(3)	16.019(3)
α (deg)	90	90	90	105.446(12)
β (deg)	103.12(3)	90	116.68(3)	103.633(14)
γ (deg)	90	90	90	90.769(13)
V (Å^3)	2372.1(8)	9621(2)	2702.1(13)	1163.9(3)
Z	4	16	4	2
D_c (g cm^{-3})	1.439	1.452	1.677	1.495
F(000)	1048	4288	1368	532
wavelength (Mo Kα (Å))	0.710 73	0.710 73	0.710 73	0.710 73
μ (mm^{-1})	1.274	1.258	1.738	1.299
crystal size (mm)	0.28 × 0.22 × 0.12	0.40 × 0.23 × 0.20	0.35 × 0.25 × 0.04	0.25 × 0.22 × 0.12
θ range (deg)	2.34−24.98	2.40−24.97	2.14−25.00	2.38−24.98
no. of total reflns collected	2190	4372	4728	4385
no. of unique reflns	2085 [*R*(int) = 0.1007]	4211 [*R*(int) = 0.0134]	4728 [*R*(int) = 0.0000]	4095 [*R*(int) = 0.0127]
no of unique reflns [$I > 2\sigma(I)$]	1783	3643	4659	3735
linear decay correction	no	no	no	no
abs. correction	*ψ* scans	*ψ* scans	DIFABS	*ψ* scans
max and min transmission	1.0000 and 0.7844	1.0000 and 0.8977	1.0000 and 0.4043	1.0000 and 0.8003
refinement method	full-matrix on F^2	full-matrix on F^2	full-matrix on F^2	full-matrix on F^2
weighting scheme	*σ* weight	*σ* weight	*σ* weight	*σ* weight
data/restraints/parameters	2085/30/211	4195/16/270	4728/20/325	4093/12/267
goodness-of-fit on F^2	1.093	1.067	1.082	1.125
final *R* indices [$I > 2\sigma(I)$]	R1 = 0.0657	R1 = 0.0278	R1 = 0.0644	R1 = 0.0321
	wR2 = 0.1804	wR2 = 0.0658	wR2 = 0.1759	wR2 = 0.0836
R indices (all data)	R1 = 0.0736	R1 = 0.0364	R1 = 0.0653	R1 = 0.0349
	wR2 = 0.1885	wR2 = 0.0879	wR2 = 0.1768	wR2 = 0.0864
largest diff peak and hole (e Å^{-3})	1.215 and −1.073	0.353 and −0.526	0.939 and −1.005	1.105 and −0.591

(m) *closo*-1-Cl-6-{Co(CO)$_2$}-2,3-(Cp*Rh)$_2$(μ_3-CO)B$_3$H$_3$, 12. 11 (0.08 g, 0.15 mmol) and $Co_2(CO)_8$ (0.08 g, 0.23 mmol) were placed in a 100 mL Schlenk tube. A 10 mL portion of freshly distilled hexane was slowly added to the mixture by syringe at −20 °C. The reaction mixture was allowed to warm to room temperature and stirred for 20 h. Insoluble black solids were removed by filtration through Celite, and column chromatography was performed at room temperature. Elution with hexane gave a brown solution ($Co_4(CO)_{12}$ by IR). Subsequent elution with ether afforded a red-orange solution, which was dried to yield 0.083 g of red-orange microcrystals of **12** (80% based on Rh). MS(EI): P^+ = 690, 3 B, 1 Cl, and 2 Rh atoms; fragment peaks corresponding to sequential loss of 3 CO; calcd for $^{12}C_{23}{}^{1}H_{33}{}^{16}O_3{}^{11}B_3{}^{59}Co^{103}Rh_2{}^{35}Cl$, 689.9853; obsd, 689.9866. NMR: ^{11}B (hexane, 22 °C), *δ* 62.8 (s, {^{1}H}, s, 1B), 37.4 (d, J_{B-H} = 150 Hz, {^{1}H}, s, 2B); ^{1}H (C_6D_6, 22 °C), *δ* 5.50 (pcq, 2H, B−H_t), 1.67 (s, 30H, C_5Me_5), −7.07 (br, 1H, B−*H*−B). IR (hexane, cm^{-1}): 2513 w (B−H); 2028 s, 1986 m, 1724 w (CO).

(n) *closo*-1-Cl-6-{Fe(CO)$_3$}-2,3-(Cp*Rh}$_2$(μ_3-CO)B$_3$H$_2$, 13. 11 (0.07 g, 0.13 mmol) and $Fe_2(CO)_9$ (0.07 g, 0.19 mmol) were placed in a 100 mL Schlenk tube. A 10 mL portion of freshly distilled hexane was slowly added to the mixture by syringe, and the reaction mixture was heated to 55 °C with stirring for 20 h. Insoluble black solids were removed by filtration through Celite, and chromatography on a silica gel plate gave 0.04 g of red microcrystals of **13** (43% based on Rh). MS(FAB): P^+ = 714, 3 B, 1 Cl, and 2 Rh atoms; fragment peaks corresponding to sequential loss of 4 CO; calcd for $^{12}C_{24}{}^{1}H_{32}{}^{16}O_4{}^{11}B_3{}^{56}Fe^{103}Rh_2{}^{35}Cl$, 713.9728; obsd, 713.9745. NMR: ^{11}B (hexane, 22 °C), *δ* 75.5 (s, {^{1}H}, s, 1B), 64.9 (d, J_{B-H} = 150 Hz, {^{1}H}, s, 2B); ^{1}H (C_6D_6, 22 °C), *δ* 8.16 (pcq, 2H, B−H_t), 1.62 (s, 30H, C_5Me_5). IR (hexane, cm^{-1}): 2450 w, 2492 w (B−H); 2028 s, 1981 m, 1965 m, 1735 m (CO).

X-ray Structure Determinations. Crystallographic information for compounds **1**−**3**, **6**, **7**, **9**, **11**, and **12** is given in Tables 1 and 2. Preliminary examination and data collection were performed with Mo Kα radiation (λ = 0.710 73 Å) on an Enraf-Nonius CAD4 computer controlled *κ* axis diffractometer equipped with a graphite crystal, incident beam monochromator at room temperature.[48] Structure solution and refinement (based on F^2) were performed on a PC by using the SHELXTL V5 package.[49] All reflections, including those with negative intensities, were included in the refinement.

(a) *nido*-1,2-(Cp*Ru)$_2$(μ-H)$_2$B$_3$H$_7$, 1. An orange blocklike crystal of **1**, obtained by keeping a saturated hexane solution at 4 °C for several days, was mounted on a glass fiber. Most of the non-hydrogen atoms were located by the direct method, and the remaining non-hydrogen atoms were found in succeeding difference Fourier syntheses. It was found that the Cp* group was disordered over two sites with occupancy coefficients of 0.5. In addition, one of the boron atoms was disordered over two sites due to the crystallographic 2-fold axis. In the final refinement, hydrogen atoms for the two sets of disordered Cp* groups were refined with an idealized riding model, which restrained the C−H distance to 0.96 Å and the isotropic thermal parameter of a hydrogen atom to 1.5 times the equivalent isotropic thermal parameter of its bonded carbon atom. The positions for the rest of the hydrogen atoms were not located and not included in the final refinement.

(b) *nido*-1,2-(Cp*Ru)$_2$(μ-H)B$_4$H$_9$, 2. A red-orange blocklike crystal, obtained by keeping a saturated hexane solution at 4 °C for several days, was mounted on a glass fiber in a random orientation. Most of the non-hydrogen atoms were located by the direct method, and the remaining non-hydrogen atoms were found in succeeding difference Fourier syntheses. In the final refinement, the Cp* hydrogen atoms were refined with an idealized riding model, which restrained the C−H distance to 0.96 Å and the isotropic thermal parameter of a hydrogen atom to 1.5 times the equivalent isotropic thermal parameter of its bonded carbon atom. After all non-hydrogen atoms were refined anisotropically and hydrogen atoms of Cp* groups refined isotropically, a difference Fourier synthesis located the rest of the hydrogen atoms, which were refined isotropically with bond length restraints.

(c) *nido*-1-(Cp*Ru)-2-(Cp*RuCO)-3-Co(CO)$_2$(μ_3-CO)B$_3$H$_6$, 3. Black platelike crystals suitable for X-ray diffraction were obtained by keeping a saturated toluene solution at 4 °C for several days, and one was mounted on a glass fiber in a random orientation. Most of the non-hydrogen atoms were located by the direct method; the remaining non-hydrogen atoms were found in succeeding difference Fourier syntheses. In the final refinement, hydrogen atoms for the Cp* groups were refined

(48) Frenz, B. A. In *The Enraf-Nonius CAD4-A Real-time System for Concurrent X-ray Data Collection and Crystal Structure Determination*; Schenk, H., Olthof-Hazelkamp, R., von Konigsveld, H., Bassi, G. C., Eds.; Delft University Press: Delft, Holland, 1978; p 64.

(49) Sheldrick, G. M. *SHELXTL V5*; Siemens Industrial Automation Inc.: Madison, WI, 1994.

Table 2. Crystallographic Data and Structure Refinement Details for Compounds **7**, **9**, **11**, and **12**

	7	**9**	**11**	**12**
empirical formula	$C_{24}H_{34}B_4FeO_4Ru_2$	$C_{20}H_{37}B_3Rh_2$	$C_{20}H_{36}B_3ClRh_2$	$C_{23}H_{33}B_3ClCoO_3Rh_2$
formula weight	687.74	515.75	550.19	690.12
crystal system	monoclinic	monoclinic	monoclinic	orthorhombic
space group	$P2_1/n$	$P2_1/c$	$P2_1/c$	$Pna2_1$
a (Å)	9.241(3)	15.2677(14)	15.574(4)	20.160(2)
b (Å)	15.112(3)	8.7342(11)	8.740(2)	9.113(2)
c (Å)	20.047(3)	17.324(2)	18.038(5)	14.544(2)
α (deg)	90	90	90	90
β (deg)	99.944(10)	103.572(9)	104.76(2)	90
γ (deg)	90	90	90	90
V (Å^3)	2757.5(11)	2245.7(4)	2374.2(10)	2672.1(6)
Z	4	4	4	4
D_c (g cm^{-3})	1.657	1.525	1.539	1.715
F(000)	1376	1048	1112	1376
wavelength (Mo Kα (Å))	0.710 73	0.710 73	0.710 73	0.710 73
μ (mm^{-1})	1.628	1.470	1.505	1.957
crystal size (mm)	0.42 × 0.30 × 0.25	0.35 × 0.28 × 0.17	0.29 × 0.18 × 0.01	0.18 × 0.11 × 0.06
θ range (deg)	2.06−24.99	2.42−24.97	2.34−24.97	2.02−24.98
no. of total reflns collected	4969	3937	4338	4702
no. of unique reflns	4828 [R(int) = 0.0383]	3937	4172 [R(int) = 0.0340]	4702
no of unique reflns [$I > 2\sigma(I)$]	4406	3619	2922	4117
decay correction	linear decay (0.0)	linear decay (0.0)	linear decay (−2.6%/63.9 h)	linear decay (0.0)
abs correction	ψ scans	DIFABS	ψ scans	ψ scans
max and min transmission	1.000 and 0.9359	1.0000 and 0.6752	0.9983 and 0.8797	0.9998 and 0.8734
data/restraints/parameters	4825/24/420	3937/11/258	4170/10/263	4702/6/311
goodness-of-fit on F^2	1.108	1.105	1.110	1.138
final R indices [$I > 2\sigma(I)$]	R1 = 0.0323	R1 = 0.0266	R1 = 0.0538	R_1 = 0.0378
	wR2 = 0.0866	wR2 = 0.0713	wR2 = 0.1191	wR2 = 0.0803
R indices (all data)	R1 = 0.0363	R1 = 0.0298	R1 = 0.0895	R1 = 0.0503
	wR2 = 0.0912	wR2 = 0.0739	wR2 = 0.1482	wR2 = 0.0902
largest diff peak and hole (e Å^{-3})	1.266 and −0.546	0.618 and −0.524	0.775 and −0.717	0.575 and −0.341

with an idealized riding model, which restrained the C−H distance to 0.96 Å and the isotropic thermal parameter of a hydrogen atom to 1.5 times the equivalent isotropic thermal parameter of its bonded carbon atom. After all non-hydrogen atoms were refined anisotropically and hydrogen atoms of Cp* groups refined isotropically, a difference Fourier synthesis located the rest of the hydrogen atoms, which were refined isotropically with bond length restraints.

(d) *pileo*-2,3-(Cp*Ru)$_2$(μ-H)B$_4$H$_7$, 6. Red-orange blocklike crystals suitable for X-ray diffraction were obtained by keeping a saturated hexane solution at 4 °C for several days, and one was mounted on a glass fiber in a random orientation. Most of the non-hydrogen atoms were located by the direct method; the remaining non-hydrogen atoms were found in succeeding difference Fourier syntheses. In the final refinement, hydrogen atoms for the Cp* groups were refined with an idealized riding model, which restrained the C−H distance to 0.96 Å and the isotropic thermal parameter of a hydrogen atom to 1.5 times the equivalent isotropic thermal parameter of its bonded carbon atom. After all non-hydrogen atoms were refined anisotropically and hydrogen atoms of Cp* groups refined isotropically, a difference Fourier synthesis located the rest of the hydrogen atoms, which were refined isotropically with bond length restraints.

(e) *pileo*-6-Fe(CO)$_3$-2,3-(Cp*Ru)$_2$(μ_3-CO)B$_4$H$_4$, 7. Red polyhedral crystals suitable for X-ray diffraction were obtained by keeping a saturated toluene solution at room temperature for 2 days, and one was mounted on a glass fiber in a random orientation. Most of the non-hydrogen atoms were located by the direct method; the remaining non-hydrogen atoms were found in succeeding difference Fourier syntheses. It was found that one of the Cp* groups was disordered over two sites with occupancy coefficients of 0.5. In the final refinement, hydrogen atoms for the Cp* groups were refined with an idealized riding model, which restrained the C−H distance to 0.96 Å and the isotropic thermal parameter of a hydrogen atom to 1.5 times the equivalent isotropic thermal parameter of its bonded carbon atom. After all non-hydrogen atoms were refined anisotropically and hydrogen atoms of Cp* groups refined isotropically, a difference Fourier synthesis located the rest of the hydrogen atoms, which were refined isotropically with bond length restraints.

(f) *nido*-2,3-(Cp*Rh)$_2$B$_3$H$_7$, 9. Dark red blocklike crystals suitable for X-ray diffraction were obtained by keeping a saturated ether solution at 4 °C for several days, and one was mounted on a glass fiber in a random orientation. Most of the non-hydrogen atoms were located by the direct method; the remaining non-hydrogen atoms were found in succeeding difference Fourier syntheses. After all non-hydrogen atoms were refined anisotropically, a difference Fourier synthesis located all hydrogen atoms. In the final refinement, Cp* hydrogen atoms were refined with an idealized riding model, which restrained the C−H distance to 0.93 Å and the isotropic thermal parameter of a hydrogen atom to 1.2 times the equivalent isotropic thermal parameter of its bonded carbon atom. The rest of the hydrogen atoms were refined isotropically with bond length restraints, which used four free variables in the refinement to confine B−H and Rh−H bond distances around their mean values.

(g) *nido*-1-Cl-2,3-(Cp*Rh)$_2$B$_3$H$_6$, 11. Red-orange crystals suitable for X-ray diffraction were obtained by keeping a saturated ether solution at −40 °C for 1 week, and one was mounted on a glass fiber in a random orientation. Most of the non-hydrogen atoms were located by the direct method, and the remaining non-hydrogen atoms were found in succeeding difference Fourier syntheses. After all non-hydrogen atoms were refined anisotropically, a difference Fourier synthesis located all hydrogen atoms. In the final refinement, cyclopentadienyl hydrogen atoms were refined with an idealized riding model, which restrained the C−H distance to 0.93 Å and the isotropic thermal parameter of a hydrogen atom to 1.2 times the equivalent isotropic thermal parameter of its bonded carbon atom. The rest of the hydrogen atoms were refined isotropically with bond length restraints, which used four free variables in the refinement to confine B−H and Rh−H bond distances around their mean values.

(h) *closo*-1-Cl-6-{Co(CO)$_2$}-2,3-(Cp*Rh)$_2$(μ_3-CO)B$_3$H$_3$, 12. Red-orange crystals suitable for X-ray diffraction were obtained by keeping a saturated ether solution at −40 °C for 1 week, and one was mounted on a glass fiber in a random orientation. Most of the non-hydrogen atoms were located by the direct method; the remaining non-hydrogen atoms were found in succeeding difference Fourier syntheses. After all non-hydrogen atoms were refined anisotropically, a difference

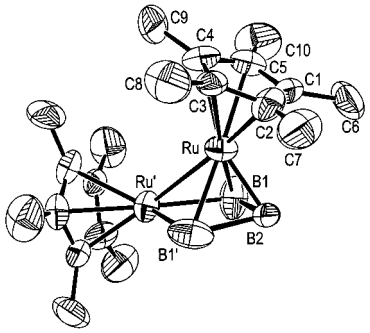

Figure 1. Molecular structure of *nido*-1,2-$(Cp^*Ru)_2(\mu\text{-}H)_2B_3H_7$, **1**. Selected bond lengths (Å) and angles (deg): Ru−Ru′ 2.814(1), Ru−B2 2.014(17), Ru−B1 2.293(12), B1−Ru1′ 2.246(10), B1−B2 1.82(2), B2−B1′ 2.02(2), B2−Ru−B1′ 56.3(6), B2−B1−Ru1′ 104.7(8), B2−B1−Ru 57.3(7), Ru1′−B1−Ru 76.6(3), B1−B2−Ru 73.2(8), B1−B2−B1′ 86.8(9), Ru−B2−B1′ 67.7(7).

Fourier synthesis located all hydrogen atoms. In the final refinement, Cp* hydrogen atoms were refined with an idealized riding model, which restrained the C−H distance to 0.93 Å and the isotropic thermal parameter of a hydrogen atom to 1.2 times the equivalent isotropic thermal parameter of its bonded carbon atom. The rest of the hydrogen atoms were refined isotropically with bond length restraints, which used four free variables in the refinement to confine B−H and Rh−H bond distances around their mean values.

Results

Synthesis of *nido*-1,2-$(Cp^*Ru)_2(\mu\text{-}H)_2B_3H_7$, 1. The reaction of $[Cp^*RuCl_2]_2$ with $[BH_4]^-$ in THF gives a single metallaborane, and the spectroscopic data support its formulation as a 7 skeletal electron pair (sep)[3,4,50] *nido*-dimetallapentaborane with the molecular formula $(Cp^*Ru)_2B_3H_9$. Although the molecules are disordered in the solid state and the hydrogen atom positions are not defined by the structure determination, the square pyramidal core geometry expected on the basis of the electron count is confirmed and the compound is identified as the 1,2-isomer (Figure 1). This core structure symmetry is consistent with the solution ^{11}B and ^1H NMR data. In addition, the ^1H NMR data reveal the presence of a pair of BHB protons, a pair of BHRu protons, and a pair of RuH protons. The first pair can only be placed on the two B−B edges of the square face, and the second logically occupies the remaining B−Ru edges of this face. This requires the third pair to be associated with the Ru centers, and we assign them as RuHRu bridging on the basis of a comparison of the chemical shift with that of the RuHRu proton of **2**. A comparison of **1** with two structurally characterized examples of 1,2- dimetallapentaboranes formed from two electron metal fragments, i.e., 1,2-$\{Fe(CO)_3\}_2B_3H_7$[51] and 1-Cp*Co-2-$\{Fe(CO)_3\}B_3H_7$,[52] shows that **1** is distinguished by the presence of two additional metal−hydride bridges.

Reaction of $[Cp^*RuCl_2]_2$ with BH_3·THF in THF yields BH_2Cl and a mixture containing **1** and **2** (see below). In contrast to the reaction with borohydride, no conditions gave pure **1**. Indeed, above room temperature and in the presence of sufficient BH_3·THF, the reaction yields product **2** directly (Scheme 1). The explanation of the differing behavior of the two monoboranes is straightforward. In our experience, borohydride reacts with available chlorides to give a simple coordinated borohydride[19] or a metallaborane containing the B_2H_6 ligand, e.g., $Cp^*_2Mo_2Cl_2B_2H_6$[20] but does not lead to cluster expansion of metallaboranes lacking halogen. Borane removes chlorides from metals as BH_2Cl[18] and adds to yield metallaboranes, but these can then undergo cluster expansion with additional borane.[53] Thus, the low selectivity of borane relative to borohydride results from competitive reaction of **1** with borane to give **2**. Experimental confirmation of this point is given in the next section.

Scheme 1

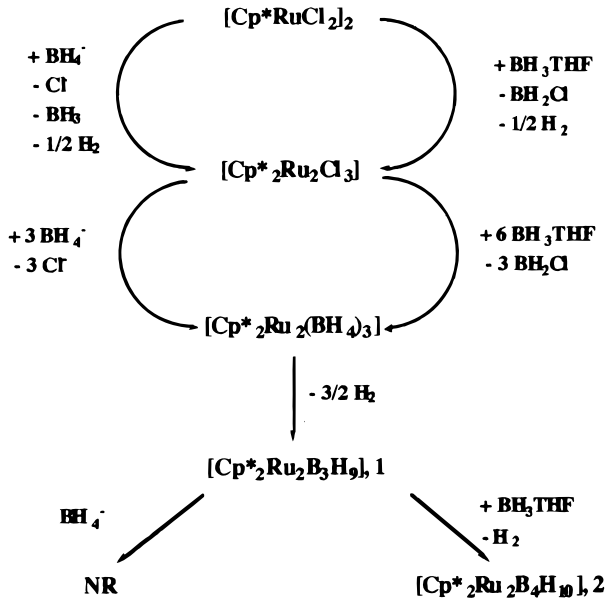

Although the first step of the reaction of monoboranes with the metal dimer is uncertain, we do know that reduction can compete with metallaborane formation.[20] Unfortunately, $[Cp^*RuCl_2]_2$ is poorly soluble under the reaction conditions, making it difficult to characterize the initial reaction. Visual observation shows that the mixed valent dimer, $[Cp^*_2Ru_2Cl_3]$, which is very soluble and highly colored, is not present in large quantities during the synthetic reaction. On the other hand, preparation of this species[46] in situ using $[Et_3BH]^-$ followed by reaction with $[BH_4]^-$ shows only the formation of **1**. As $[Cp^*RuCl]_4$ is also poorly soluble and, in any case, is not expected to give **1** upon treatment with $[BH_4]^-$, we suggest that the reaction proceeds through the mixed-valent chloride dimer and a ruthenium borohydride as low concentration intermediates as shown in Scheme 1. Loss of hydrogen from the ruthenium borohydride with M−B and B−B bond formation leads to the first observed product **1**. Addition of BH_3·THF to give **2** is facile (see below) whereas further reaction with $Li[BH_4]$ is not.

Syntheses of $(Cp^*Rh)_2B_2H_6$, 8, and *nido*-2,3-$(Cp^*Rh)_2B_3H_7$, 9. Reaction of $[Cp^*RhCl_2]_2$ with $Li[BH_4]$ at room temperature produces a single metallaborane (Scheme 2). Although we were unable to obtain single crystals suitable for a structure determination, the spectroscopic data unambiguously show the compound to be $(Cp^*Rh)_2B_2H_6$, **8**, a rhodium dimer perpendicularly bridged by an ethane-like B_2H_6 ligand (Figure 2). That is, the high-resolution mass data establish the molecular formula, the ^{11}B NMR spectrum shows equivalent borons, and the proton NMR spectrum shows signals due to Cp* ligands, BH terminal protons, and RhHB bridging protons in the ratio of 15:1:2. There are now several known examples of species such as **8** which contain formal $[B_2H_6]^{2-}$ ligands in one of two tautomeric forms, and four have been crystallographically characterized.[20−22,54]

(50) Wade, K. *Electron Deficient Compounds*; Nelson: London, 1971.
(51) Andersen, E. L.; Haller, K. J.; Fehlner, T. P. *J. Am. Chem. Soc.* **1979**, *101*, 4390.
(52) Lei, X.; Shang, M.; Fehlner, T. P. *Organometallics* **1998**, *17*, 1558.
(53) Aldridge, S.; Hashimoto, H.; Kawamura, K.; Shang, M.; Fehlner, T. P. *Inorg. Chem.* **1998**, *37*, 928.
(54) Cotton, F. A.; Daniels, L. M.; Murillo, C. A.; Wang, X. *J. Am. Chem. Soc.* **1996**, *118*, 4830.

Scheme 2

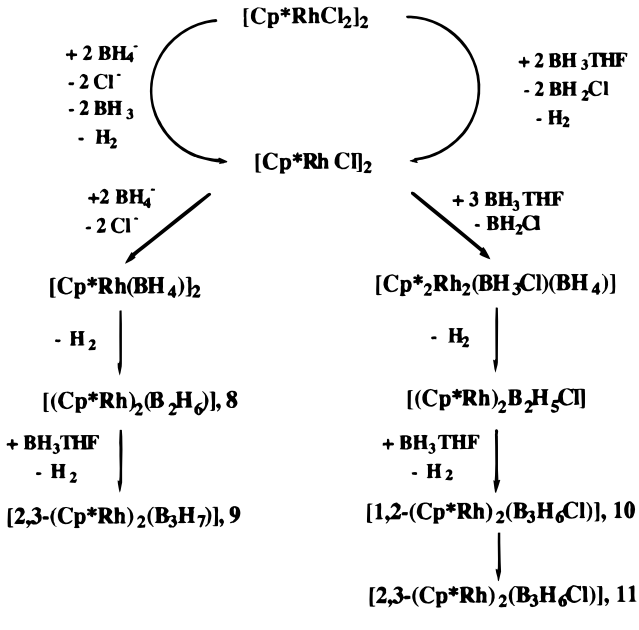

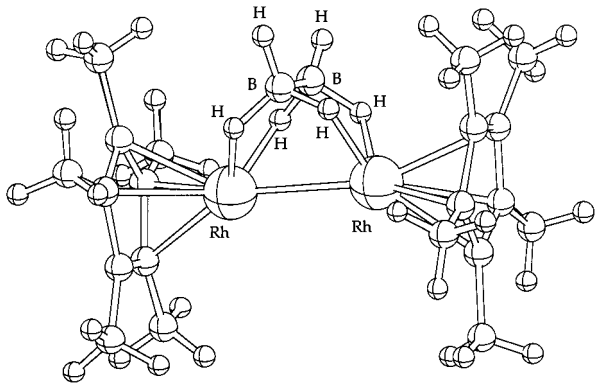

Figure 2. Proposed structure of $(Cp^*Rh)_2B_2H_6$, **8**.

Compound **8** reacts with BH_3·THF at elevated temperature to yield one major metallaborane product but in a mixture with significant amounts of two additional species. Isolated by fractional crystallization, the major product is 7-sep *nido*-2,3-$(Cp^*Rh)_2B_3H_7$, **9** (Scheme 3). Both the spectroscopic data and solid-state structure (Figure 2) define the structure as a square pyramidal dimetallaborane, but in contrast to those of **1**, both metal atoms are found in basal positions. Thus, it constitutes a homometallic example analogous to 2-(Cp*Ir)-3-{$(PPh_3)_2(CO)$-Os}B_3H_7.[55] The route to **9** is not as selective as one would wish, and the chloro derivative **11**, isolated in better yield without painstaking separation (see below), provides a more convenient platform for the investigation of reaction chemistry.

Syntheses of *nido*-3-Cl-1,2-$(Cp^*Rh)_2B_3H_6$, 10, and *nido*-1-Cl-2,3-$(Cp^*Rh)_2B_3H_6$, 11. The reaction of $[Cp^*RhCl_2]_2$ with BH_3·THF at 60 °C results in the formation of a single metallaborane which can be isolated in high yield. The new compound is identified as 7-sep *nido*-1-Cl-2,3-$(Cp^*Rh)_2B_3H_6$, **11** (Schemes 2 and 3), on the basis of its spectroscopic properties and solid-state structure (Figure 3).[36] It is isostructural with **9** and differs only in the substitution of the terminal hydrogen on the apical boron atom with a chlorine atom (Figure 2). Cl substitution for H appears to be a minor structural perturbation.

At room temperature and relatively short reaction times, only small amounts of **11** are observed and the major product is a different compound which is identified as 7-sep *nido*-3-Cl-1,2-$(Cp^*Rh)_2B_3H_6$, **10** (Figure 4, Schemes 2 and 3), on the basis of a comparison of its spectroscopic data with those of **9** and **11**. Curiously, one of the four cluster bridging hydrogens bridges the apical and basal Rh atoms rather than an edge of the open square face as found in B_5H_9 itself. However, the distinctly broadened line width of the triplet associated with this proton shows it to be associated with, if not bonded to, the adjacent boron atom. At 60 °C, pure **10** cleanly isomerizes to **11**, and this reaction constitutes a rare example of a metallaborane cluster isomerization. Further, it demonstrates kinetic control of the reaction system and a greater thermodynamic stability for the 2,3-isomer relative to the 1,2-isomer. As we find no evidence for thermal rearrangement of **1**, the difference in isomer stabilities is attributed to the accommodation of RuH vs Rh in a *nido*-M_2B_3 cluster.

Reaction of $[Cp^*RhCl_2]_2$ with BH_3·THF in THF at room temperature results in a change in color from orange of the suspension to the characteristic blue of $[Cp^*RhCl]_2$,[56] showing that reduction precedes metallaborane formation. The color change is accompanied by the formation of BH_2Cl and a gas, presumably H_2. On continued reaction, the blue color changes to red-orange, additional BH_2Cl is formed, and a metallaborane product is observed. No similar color change is observed for the reaction of $[Cp^*RhCl_2]_2$ with $Li[BH_4]$, probably because the steady-state concentration of $[Cp^*RhCl]_2$ never reaches a high enough level for visual observation. The fact that no $(Cp^*RhCl)_2B_2H_6$ or $(Cp^*Rh)_2(B_2H_6)_2$, analogous to $(Cp^*MoCl)_2B_2H_6$ or $(Cp^*Mo)_2(B_2H_6)_2$ formed in the reaction of $\{Cp^*MoCl_2\}_2$ with 2 $Li[BH_4]$ and 4 $Li[BH_4]$, respectively,[20] is observed is also consistent with reduction followed by metallaborane formation as shown in Scheme 2.

The incorporation of Cl in the borane pathway suggests a competition between H_2 loss with concomitant BB bond formation in an intermediate chloroborohydride complex and exchange of the last Cl atom between free borane and the complex. Note that a mononuclear chlorohydride ruthenium complex was recently reported.[28] Also, chloroborohydride metal salts are known and have been structurally characterized.[57] Exchange between a coordinated chloroborohydride and free borane could easily proceed via a pathway analogous to that found for the redistribution reaction of haloboranes with boranes.[58] For rhodium, but thus far for no other metal, hydrogen elimination to give the chlorine-substituted dirhodaborane intermediate $(Cp^*Rh)_2B_2H_5Cl$ dominates the exhange of the chlorine with the chloroborohydride to give $(Cp^*Rh)_2B_2H_6$, **8**. The former leads to **10** and then **11**, whereas the latter would give **9**, which is not observed. Consistent with this hypothesis, spectroscopic evidence for small amounts of a dichloro analogue of **11** was observed.

Cluster Expansion of *nido*-1,2-$(Cp^*Ru)_2(\mu\text{-}H)_2B_3H_7$, 1. The reaction of pure **1** with BH_3·THF results in a facile and quantitative conversion to a single compound. On the basis of spectroscopic data, this compound is an 8-sep *nido*-dimetallahexaborane and demonstrates that cluster expansion by the formal insertion of a BH fragment into **1** has taken place. A solid-state structure determination (Figure 5) shows that the new metallaborane is *nido*-1,2-$(Cp^*Ru)_2(\mu\text{-}H)B_4H_9$, **2**, in which the core geometry and the skeletal hydrogen atom positions are in accord with the solution NMR data.

(55) Bould, J.; Pasieka, M.; Braddock-Wilking, J.; Rath, N. P.; Barton, L.; Gloeckner, C. *Organometallics* **1995**, *14*, 5138.

(56) Sharp, P. R.; Hoard, D. W.; Barnes, C. L. *J. Am. Chem. Soc.* **1990**, *112*, 2024.

(57) Lawrence, S. H.; Shore, S. G.; Koetzle, T. F.; Huffman, J. C.; Wei, C.-Y.; Bau, R. *Inorg. Chem.* **1985**, *24*, 3171.

(58) Onak, T. *Organoborane Chemistry*; Academic Press: New York, 1975.

Scheme 3

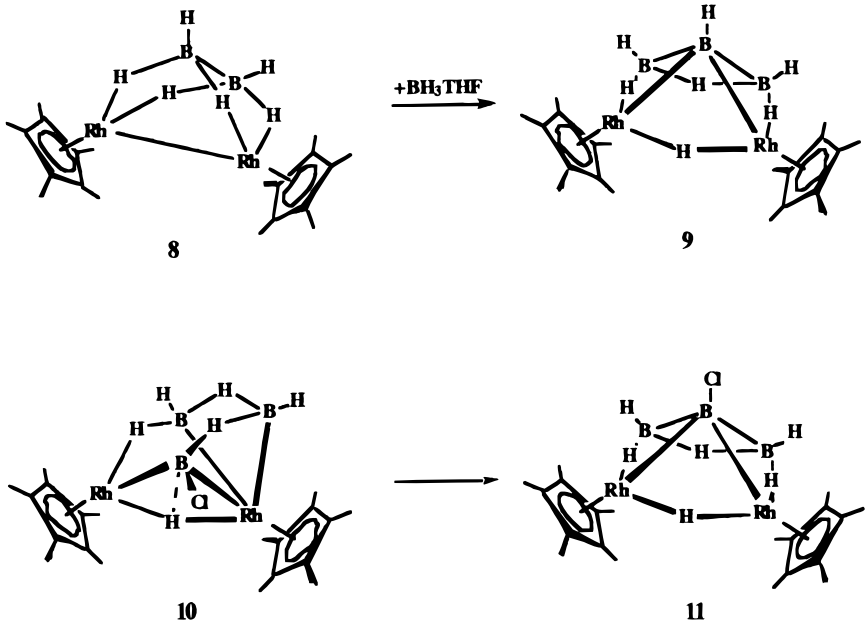

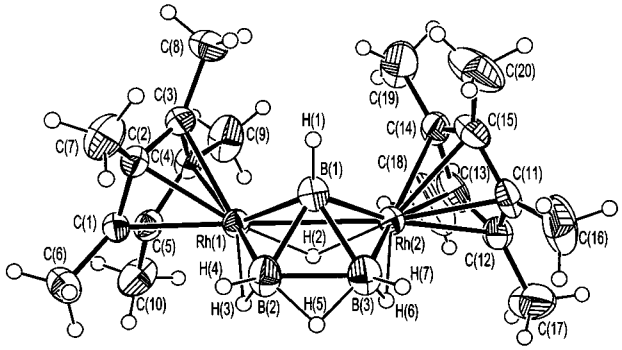

Figure 3. Molecular structure of *nido*-2,3-$(Cp^*Rh)_2B_3H_7$, **9**. Note that **9** is isostructural with *nido*-1-Cl-2,3-$(Cp^*Rh)_2B_3H_6$, **11**.[36] Selected bond lengths (Å) and angles (deg) for **9**: Rh1−Rh2 2.8491(4), Rh1−B1 2.112(4), Rh1−B2 2.188(4), Rh2−B1 2.114(4), Rh2−B3 2.198(4), B1−B2 1.741(6), B1−B3 1.756(6), B2−B3 1.758(6), B1−Rh1−B2 47.7(2), B2−Rh1−Rh2 75.54(11), B2−B1−B3 60.4(2), B3−B1−Rh1 108.0(3), B3−B1−Rh2 68.5(2), Rh1−B1−Rh2 84.79(13), B1−B2−B3 60.3(2), B3−B2−Rh1 104.8(2), B2−B3−Rh2 104.0(2).

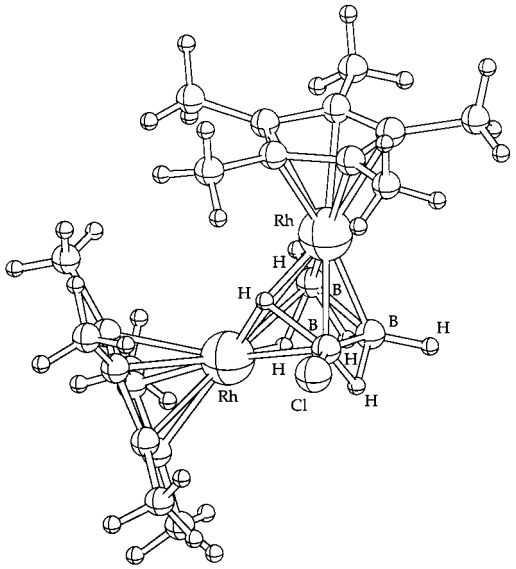

Figure 4. Proposed structure of *nido*-3-Cl-1,2-$(Cp^*Rh)_2B_3H_6$, **10**.

Examples of monometallahexaboranes are known, e.g., 2-$(CO)_3FeB_5H_9$ (Chart 1).[59] But cluster **2** is the first example of a structurally characterized dimetallahexaborane analogous to B_6H_{10} in which the apical BH and a basal BH are subrogated by Cp*RuH; i.e., in contrast to a hypothetical *nido*-1,2-$\{(CO)_3Fe\}_2B_4H_8$ dimetallahexaborane (Chart 1), **2** possesses two additional endo hydrogen atoms. Thus, all five edges of the pentagonal open face are bridged by hydrogen atoms as is the Ru−Ru apical−basal edge. Note that **2** is closely related to the organometallic "ferrole" $Fe_2(CO)_6C_4H_4$ and is a metallaborane analogue of $Cp^*Cl_2Ru(\eta^2{:}\eta^4\text{-}\mu_2\text{-}C_4H_4)RuCp^*$.[60]

The clean conversion of **1** to **2** confirms the cluster expansion step incorporated into the pathway given in Scheme 1. Although the reaction of **1** with excess $[BH_4]^-$ at 60 °C also produces some **2**, the reaction is much slower than that with BH_3·THF and requires elevated temperatures. Slow formation of borane from the borohydride would account for the **2** observed.

Chart 1

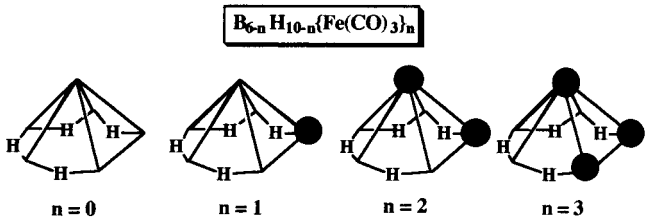

Compound **1** also reacts with $Co_2(CO)_8$ at room temperature to give a single metallaborane in good yield. Spectroscopic data suggests addition of the components of $Co(CO)_4$ accompanied by the loss of hydrogen. Spectroscopic and crystallographic characterizations combined define the new compound as the 8-sep trimetallic cluster *nido*-1-(Cp*Ru)-2-(Cp*RuCO)-3-Co-$(CO)_2(\mu_3\text{−}CO)B_3H_6$, **3** (Figure 6). Like **2**, **3** can be considered a metal analogue of B_6H_{10} but one in which an apical and two adjacent basal BH fragments are subrogated by metal fragments as in the hypothetical 1,2,3-$\{(CO)_3Fe\}_3B_3H_7$ (Chart 1).

(59) Shore, S. G.; Raganini, D.; Smith, R. L.; Cottrell, C. E.; Fehlner, T. P. *Inorg. Chem.* **1979**, *18*, 670.

(60) Campion, B. K.; Heyn, R. H.; Tilley, T. D. *Organometallics* **1990**, *9*, 1106.

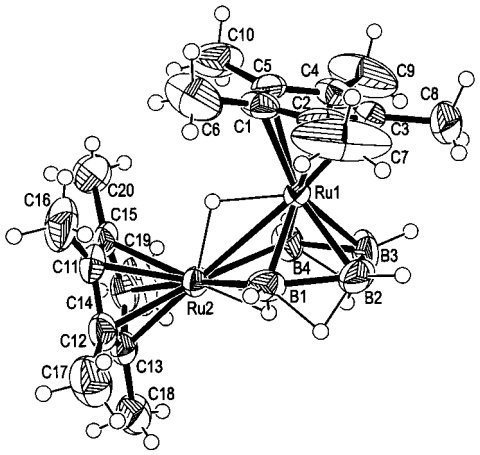

Figure 5. Molecular structure of *nido*-1,2-$(Cp^*Ru)_2(\mu\text{-}H)B_4H_9$, **2**. Selected bond lengths (Å) and angles (deg): Ru1−Ru2 2.8527(4), Ru1−B2 2.121(5), Ru1−B3 2.122(5), Ru1−B1 2.167(5), Ru1−B4 2.169(5), Ru2−B4 2.317(5), Ru2−B1 2.321(5), B1−B2 1.831(8), B2−B3 1.784(11), B3−B4 1.805(9), B4−Ru2−Ru1 48.26(13), B1−Ru2−Ru1 48.19(13), B2−Ru1−B1 50.5(2), B3−Ru1−B1 87.4(3), B2−Ru1−B4 86.9(3), B3−Ru1−B4 49.7(2), B1−Ru1−B4 89.3(2), B4−Ru2−B1 82.2(2), B2−B1−Ru2 117.1(4), B3−B2−B1 110.1(4), B2−B3−B4 110.6(4), B3−B4−Ru2 117.8(4).

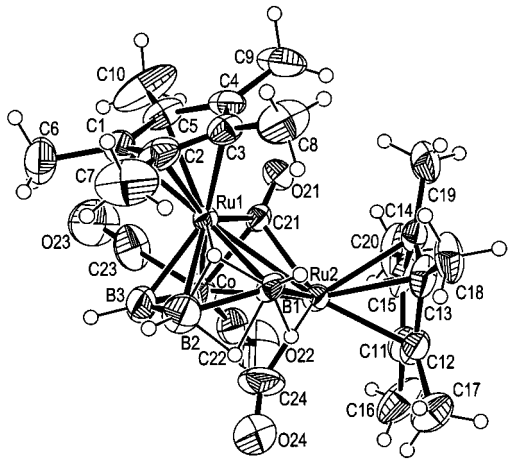

Figure 6. Molecular structure of *nido*-1-(Cp*Ru)-2-(Cp*RuCO)-3-$Co(CO)_2(\mu_3\text{-}CO)B_3H_6$, **3**. Selected bond lengths (Å) and angles (deg): Ru1−Ru2 2.8155(13), Ru1−Co 2.597(2), Ru2−Co 2.648(2), Ru1−B1 2.09(2), Ru1−B2 2.18(2), Ru1−B3 2.09(3), Ru1−C21 2.121(13), Ru2−B1 2.146(13), Ru2−C21 2.178(13), Ru2−C24 2.00(2), Co−B3 2.25(3), Co−C21 1.903(13), Co−C22 1.73(2), Co−C23 1.82(2), Co−C24 2.42(2), B1−B2 1.76(3), B2−B3 1.62(4), Co−Ru1−Ru2 58.41(6), B1−Ru1−B3 85.1(8), B1−Ru1−B2 48.6(7), B3−Ru1−B2 44.5(12), B1−Ru2−Co 92.9(5), B3−Co−Ru2 90.6(7), B2−B3−Co 120.0(13), B3−B2−B1 114(2), B2−B1−Ru2 116.4(12).

Curiously, **3** contains a $Co(CO)_2$ fragment, a CO ligand triply bridging the Ru_2Co face, and a nearly terminal CO attached to the basal Ru atom. Selective $^1H\{^{11}B\}$NMR experiments verify the most surprising feature of its solid state structure—one basal BH fragment is left completely unbridged and the missing hydrogen ends up triply bridging a RuB_2 face. The chemical shift of this bridging hydrogen is likewise very unusual, being 3.2 ppm downfield of the B−H−B proton. In a normal *nido*-borane, the endo hydrogen found bridging the Ru(1)−B(1)−B(2) face would be expected to be bridging the B(2)−B(3) edge. As there are alternative positions to place this particular hydrogen on the cluster, its observed location suggests that each one-electron Cp*Ru fragment demands an associated H atom. This consistent with the hydrogen atom locations of **1** and **2** above although in these cases there were no obvious alternatives for the placement of the extra hydrogens. The observed distribution of endo hydrogens on **3** can be taken to reflect the framework charge distribution perturbed by the requirements of the metal fragments.[61]

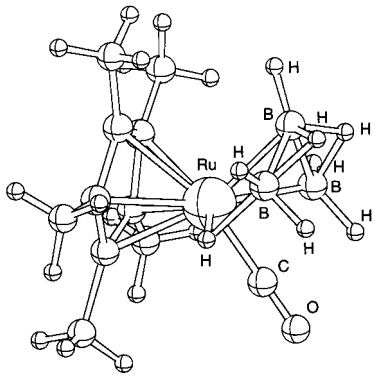

Figure 7. Proposed structure of *arachno*-$(Cp^*Ru)(CO)(\mu\text{-}H)B_3H_7$, **4**.

A ^{11}B NMR study showed that **1** does react with $Fe_2(CO)_9$ but yields only small amounts of boron-containing species. It completely decomposes to intractible material when heated to 80 °C for 20 h.

Degradation of *nido*-1,2-$(Cp^*Ru)_2(\mu\text{-}H)_2B_3H_7$, 1. The reaction of **1** with excess $Co_2(CO)_8$ cleanly results in **3**; however, small amounts of a second product were observed in the ^{11}B NMR spectra. Addition of 1 equiv of $Co_2(CO)_8$ under more dilute conditions gave an increased yield of this other species, permitting its isolation even though **3** remained the major product. The spectroscopic data allow unambiguous identification of the new compound as *arachno*-$(Cp^*Ru)(CO)(\mu\text{-}H)B_3H_7$, **4** (Figure 7), a new "borallyl" metal complex related to the many borallyl complexes already known (Co[52] , Ir,[62,63] Pd,[64,65] and Pt[66−68]). This additional reaction pathway is that observed exclusively in the reaction of *nido*-2,4-$(Cp^*Co)_2B_3H_7$ with $Co_2(CO)_8$ to give *arachno*-$(Cp^*Co)(CO)B_3H_7$.[52] Thus, the sensitivity of the reaction of **1** with $Co_2(CO)_8$ to reaction conditions is mechanistically significant (see below).

Dehydrogenation of *nido*-1-(Cp*Ru)-2-(Cp*RuCO)-3-$Co(CO)_2(\mu_3\text{-}CO)B_3H_6$, 3. The mild pyrolysis of **3** results in the clean conversion to a new metallaborane. The mass spectrometric data show the loss of two hydrogen atoms from **3**, and the IR spectrum confirms the retention of the triply bridging CO ligand and the $Co(CO)_2$ fragment of **3** as well as the presence of another bridging CO. The ^{11}B NMR indicates the existence of a plane of symmetry in the molecule, which is confirmed by the observation of a single Cp* methyl resonance in the ^1H NMR. Consistent with the molecular formula derived from the mass data, a single skeletal hydrogen is observed in the ^1H NMR with a peak width and a chemical shift consistent with association with the quadrupolar Co atom. Thus, the

(61) Fehlner, T. P. *Polyhedron* **1990**, *9*, 1955.
(62) Greenwood, N. N.; Kennedy, J. D.; Reed, D. *J. Chem. Soc.,Dalton Trans.* **1980**, 196.
(63) Bould, J.; Greenwood, N. N.; Kennedy, J. D.; McDonald, W. S. *J. Chem. Soc., Dalton Trans.* **1985**, 1843.
(64) Housecroft, C. E.; Shaykh, B. A. M.; Rheingold, A. L.; Haggerty, B. S. *Inorg. Chem.* **1991**, *30*, 125.
(65) Housecroft, C. E.; Owen, S. M.; Raithby, P. R.; Shaykh, B. A. M. *Organometallics* **1990**, *9*, 1617.
(66) Bould, J.; Kennedy, J. D.; Mcdonald, W. S. *Inorg. Chim. Acta* **1992**, *196*, 201.
(67) Guggenberger, L. J.; Kane, A. R.; Muetterties, E. L. *J. Am. Chem. Soc.* **1972**, *94*, 5665.
(68) Haggerty, B. S.; Housecroft, C. E.; Rheingold, A. L.; Shaykh, B. A. M. *J. Chem. Soc., Dalton Trans.* **1991**, 2175.

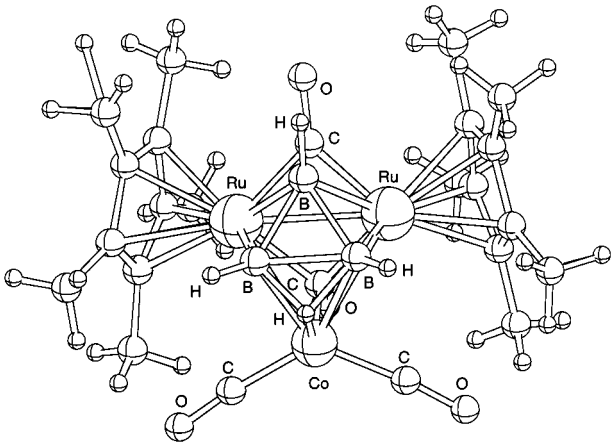

Figure 8. Proposed structure of *closo*-6-Co(CO)$_2$-2,3-(Cp*Ru)$_2$(μ-CO)-(μ_3-CO)B$_3$H$_4$, **5**.

compound is formulated as a 7-sep M_3B_3 octahedral cluster, *closo*-6-Co(CO)$_2$-2,3-(Cp*Ru)$_2$(μ-CO)(μ_3-CO)B$_3$H$_4$, **5**, and the proposed structure is shown in Figure 8. It is a member of a small class of such compounds,[69−72] and there is a close relationship between the proposed structure of **5** and the observed structures of compounds **7** and **12**, discussed below.

Dehydrogenation of *nido*-1,2-(Cp*Ru)$_2$(μ-H)B$_4$H$_9$, 2. Attempts to react **2** further with BH$_3$·THF or with either Co$_2$(CO)$_8$ or Fe$_2$(CO)$_9$ only gave unreacted **2** despite temperatures up to 80 °C and long reaction times. However, at 90 °C, a new compound was observed in the ^{11}B NMR spectra of the reaction mixture. Subsequently, it was found that this compound could be generated quantitatively by simply heating a solution of **2** at 95 °C. The spectroscopic data showed that **2** had lost two hydrogen atoms, presumably as H$_2$, suggesting a six-atom, 7-sep cluster product. However, these data are not easily accommodated by a closo cluster structure and a solid-state structure determination revealed the product to be *pileo*-2,3-(Cp*Ru)$_2$-(μ-H)B$_4$H$_7$, **6**, with a BH-capped *nido*-2,3-(Cp*Ru)$_2$B$_3$H$_7$ structure (Figure 9). As such, it is the dimetal analogue of *pileo*-1,2,3-(Cp*Ru)$_3$(μ-H)B$_3$H$_7$ formed as a minor byproduct in the synthesis of **1**.[73]

The square pyramidal framework of **6** is similar to that observed for **9**, but **6** possesses an added BH fragment which caps the M$_2$B face. Again, each Cp*Ru fragment is associated with a hydrogen atom; however, there is nothing unusual about the placement of these atoms on the cluster framework. This is the second example of a capped dimetallapentaborane to be reported. The first is *pileo*-2,3-{(PMe$_3$)$_2$HFe}$_2$B$_4$H$_8$ isolated in 1% yield from the reaction of Fe(PMe$_3$)$_3$(η^2-CH$_2$PMe$_2$)H with B$_5$H$_9$.[74] The synthetic advantage using monoboranes to build a metallaborane on a dimetal species in this case corresponds to a factor of 76 in yield even though the route involves three separate steps.

Metal Fragment Addition to *pileo*-2,3-(Cp*Ru)$_2$(μ-H)B$_4$H$_7$, 6. Heating **6** in the solid state under vacuum to higher temperatures only resulted in sublimation of **6** accompanied by some decomposition to intractible material. Likewise, treatment with BH$_3$·THF up to 100 °C gave no reaction. However, **6** reacts cleanly with Fe$_2$(CO)$_9$ to give a single metallaborane in good yield. The spectroscopic data showed the addition of the elements of Fe(CO)$_4$ and the loss of four hydrogen atoms, suggesting a seven-vertex, 7-sep cluster product. The capped closo cluster structure suggested by the NMR data was confirmed by a solid-state structure determination as *pileo*-6-Fe(CO)$_3$-2,3-(Cp*Ru)$_2$(μ_3-CO)B$_4$H$_4$, **7** (Figure 10). The Fe(CO)$_3$ fragment formally replaces two endo hydrogens, and the CO ligand triply bridging the trimetal face replaces the other two. The capping BH fragment retains its position on the Ru$_2$B face as found in **6**. Presumably, the incoming metal fragment interacts with the square face of **6,** leaving the remainder of the cluster intact. The existing example of a capped trimetal octahedral

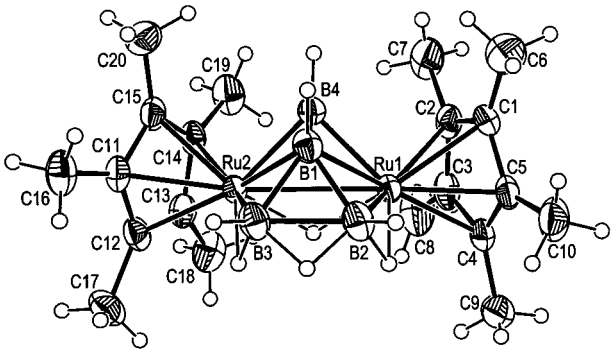

Figure 9. Molecular structure of *pileo*-2,3-(Cp*Ru)$_2$(μ-H)B$_4$H$_7$, **6**. Selected bond lengths (Å) and angles (deg): Ru1−Ru2 2.8550(7), Ru1−B4 2.038(5), Ru1−B2 2.210(5), Ru1−B1 2.235(5), Ru2−B4, 2.047(5), Ru2−B3 2.226(5), Ru2−B1 2.243(5), B1−B3 1.717(7), B1−B2 1.719(8) B1−B4 1.740(7), B2−B3 1.834(8), B4−Ru1−B2 93.2(2), B2−Ru1−Ru2 76.76(14), B4−Ru2−B3 92.7(2), B4−Ru2−B1 47.6(2), B3−Ru2−Ru1 76.63(14), B3−B1−B2 64.5(3), B3−B1−B4 127.0(4), B2−B1−B4 126.4(4), B3−B1−Ru1 106.8(3), Ru1−B1−Ru2 79.2(2), B1−B2−B3 57.7(3), B3−B2−Ru1 103.7(3), B2−B3−Ru2 102.9(3), B1−B4−Ru1 72.0(2), B1−B4−Ru2 72.1(2), Ru1−B4−Ru2 88.7(2).

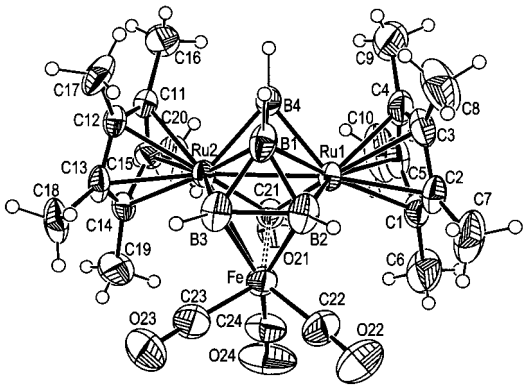

Figure 10. Molecular structure of *pileo*-6-Fe(CO)$_3$-2,3-(Cp*Ru)$_2$(μ_3-CO)B$_4$H$_4$, **7**. Selected bond lengths (Å) and angles (deg): Ru1−Ru2 2.6816(5), Ru1−Fe 2.7178(9), Ru2−Fe 2.709(1), Ru1−C(21) 2.045(4), Ru1−B4 2.068(5), Ru1−B2 2.161(5), Ru1−B1 2.220(5), Ru2−C(21) 2.047(4), Ru2−B4 2.066(5), Ru2−B3 2.162(5), Ru2−B1 2.232(5), Fe−C22 1.750(6), Fe−C23 1.765(6), Fe−C24 1.810(7), Fe−B3 2.083(6), Fe−B2 2.086(6), Fe−C(21) 2.492(4), B1−B2 1.712(9), B1−B3 1.715(9), B1−B4 1.773(8), B2−B3 1.772(8), C21−Ru1−B4 85.7(2), C21−Ru1−B2 107.0(2), B4−Ru1−B2 94.6(2), B2−Ru1−Ru2 77.90(14), C21−Ru1−Fe 61.16(13), B4−Ru1−Fe 106.40(14), C(21)−Ru2-B4 85.7(2), C(21)−Ru2−B3 107.0(2), B4−Ru2−B3 94.4(2), B2−B1−B4 126.2(4), B3−B1−Ru1 101.7(3), B2−B1−Ru2 101.5(3), B1−B2−B3 59.0(3), B1−B2−Fe 105.0(3), B3−B2−Ru1 102.1(3), B1−B3−Fe 105.0(3), B2−B3−Ru2 102.2(3), Ru2−B4−Ru1 80.9(2).

(69) Zimmerman, G. J.; Hall, L. W.; Sneddon, L. G. *Inorg. Chem.* **1980**, *19*, 3642.
(70) Miller, V. R.; Weiss, R.; Grimes, R. N. *J. Am. Chem. Soc.* **1977**, *99*, 5646.
(71) Pipal, J. R.; Grimes, R. N. *Inorg. Chem.* **1977**, *16*, 3255.
(72) Weiss, R.; Bowser, J. R.; Grimes, R. N. *Inorg. Chem.* **1978**, *17*, 1522.
(73) Lei, X.; Shang, M.; Fehlner, T. P. *Inorg. Chem.* **1998**, *37*, 3900.
(74) Grebenik, P. D.; Green, M. L. H.; Kelland, M. A.; Leach, J. B.; Mountford, P. *J. Chem. Soc., Chem. Commun.* **1990**, 1234.

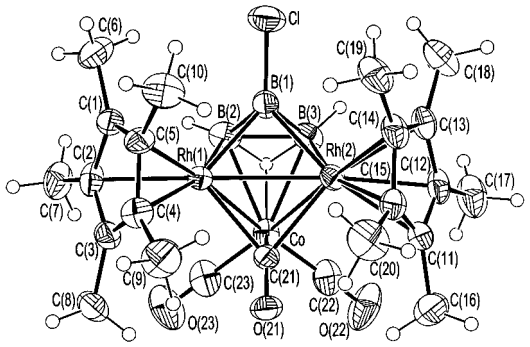

Figure 11. Molecular structure of *closo*-1-Cl-6-{$Co(CO)_2$}-2,3-$(Cp^*Rh)_2(\mu_3\text{-}CO)B_3H_3$, **12.** Selected bond lengths (Å) and angles (deg): Rh1−Co 2.5450(12), Rh2−Co 2.5465(11), Rh1−Rh2 2.7070(8), Rh1−B1 2.114(10), Rh1−B2 2.170(10), Rh2−B1 2.125(9), Rh2−B3 2.152(9), Co−B2 2.240(11), Co−B3 2.225(12), B1−Cl 1.805(11), B1−B2 1.70(2), B1−B3 1.71(2), B2−B3 1.77(2), Co−Rh1−Rh2 57.91(3), B1−Rh2−B3 47.2(4), B1−Rh2−Rh1 50.1(3), Co−Rh2−Rh1 57.85(3), B1−B2−B3 59.2(6), B2−B1−B3 62.4(7), B2−B1−Rh1 68.4(5), B3−B1−Rh1 106.3(6), Rh1−B1−Rh2 79.4(3), B1−B2−Co 95.7(6).

metallaborane, *pileo*-1,2,3-$(Cp^*Co)_3B_4H_4$,[75,76] displays a BH cap on the triangular Co_3 face. Compound **6** also reacts with $Co_2(CO)_8$ but gives more than two compounds in low yields on the basis of ^{11}B NMR spectroscopy.

Metal Fragment Addition to *nido*-1-Cl-2,3-$(Cp^*Rh)_2B_3H_6$, 11. Reaction of **11** with $Co_2(CO)_8$ at room temperature results in the formation of a single metallaborane product isolated in good yield. Spectroscopic characterization in solution and a solid-state structure determination define the cluster product as 7-sep *closo*-1-Cl-6-{$Co(CO)_2$}-2,3-$(Cp^*Rh)_2(\mu_3\text{-}CO)B_3H_3$, **12** (Figure 11). As noted already, there are examples of homometallic M_3B_3 octahedral cluster structures known,[69−72] but **5** and **12** are the first examples derived from directed syntheses.

In contrast to metal fragment additions to **1** and **6**, **11** also reacts cleanly with $Fe_2(CO)_9$ to give a single metallaborane product. Although a solid-state structure was not obtained, the spectroscopic data show it to be a close analogue of **12**, namely, 7-sep *closo*-1-Cl-6-{$Fe(CO)_3$}-2,3-$(Cp^*Rh)_2(\mu_3\text{-}CO)B_3H_2$, **13**. The exact mass establishes the molecular formula, the ^1H and ^{11}B NMR spectra reveal a plane of symmetry, and the IR data suggest the presence of an $Fe(CO)_3$ fragment plus a μ_3-CO ligand. Thus, we propose the structure shown in Figure 12, in which the iron fragment has simply added to the square base of **11** in the same manner as the cobalt fragment. This structure also contains a triangular metal fragment to support the triply bridging carbonyl ligand. The difference between **12** and **13** is the presence of a CoH moiety in the former vs Fe(CO) in the latter.

Discussion

Formation of M−B Bonds. Pathways for the formation of the M_2B_3 clusters of Ru and Rh are given in Schemes 1 and 2. They conforms in general to past experience with Co,[18] Cr,[19] and Mo;[20] however each metal exhibits unique aspects associated with the competition among formal reduction of the monocyclopentadienylmetal chloride, formation of M−B and B−B bonds, and cluster expansion by borane. That is, reaction of the monocyclopentadienylmetal chloride with borohydride yields a metal borohydride (Cr) or a metal dimer with a formal $[B_2H_6]^{2-}$ ligand bridging the metal−metal bond (Co, Mo). Here,

(75) Venable, T. L.; Grimes, R. N. *Inorg. Chem.* **1982**, *21*, 887.
(76) Venable, T. L.; Sinn, E.; Grimes, R. N. *Inorg. Chem.* **1982**, *21*, 904.

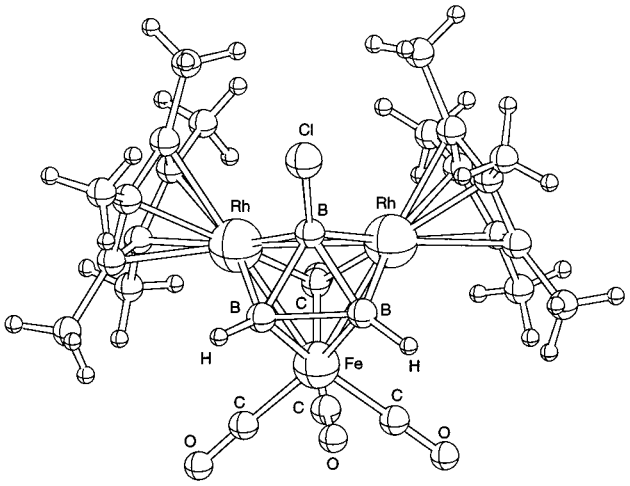

Figure 12. Proposed structure of *closo*-1-Cl-6-{$Fe(CO)_3$}-2,3-$(Cp^*Rh)_2(\mu_3\text{-}CO)B_3H_2$, **13**.

Scheme 4

$[Cp^*MCl]_2 \xrightarrow[\text{Co, Rh}]{} [(Cp^*M)_2(B_2H_6)]$
$\downarrow$ Rh
$[(Cp^*M)_2(B_3H_7)]$
$\downarrow$ Ru
$[(Cp^*M)_2(B_4H_8)]$
$\downarrow$ Cr
$[(Cp^*M)_2(B_5H_9)]$

Rh behaves like Co whereas Ru yields a M_2B_3 product directly from the mixed-valent dimer. Reaction with borane and elimination of BH_2Cl lead directly to a M_2B_3 cluster (Co) or a M_2B_5 cluster (Mo) although considerable manipulation of the reaction system to yield other products is possible for the latter metal. $[Cp^*CrCl]_2$ is an exception in that the formation of a M_2B_4 cluster is accompanied by the formation of $[Cp^*CrCl_2]_2$ rather than BH_2Cl. With borane, both Rh and Ru generate BH_2Cl and form M_2B_3 clusters. For Rh, chlorine removal as BH_2Cl is less efficient and the major M_2B_3 product contains a chlorine atom. For Ru, the M_2B_3 to M_2B_4 expansion reaction is competitive with M_2B_3 formation.

Cluster Expansion. Generally, dimeric monocyclopentadienylmetal chlorides give dimetallaboranes as the principal product, but the number of borane fragments in the cluster depends on the metal and the monoborane used. E.g., for M_2B_n: Co, $n = 3$;[18] Cr, $n = 4$;[19] Mo, $n = 5$.[20] A stepwise buildup of M_2B_n from a $M_2B_2H_6$ intermediate is very appealing. In the present work, we have established examples of cluster expansion for M_2B_2 to M_2B_3 and M_2B_3 to M_2B_4. As we have previously reported the M_2B_4 to M_2B_5 step for M = Cr,[53] prototypes for a stepwise assembly of all the dimetallaboranes observed now exist (Scheme 4, where the metals on each arrow refer to the metals for which examples of the cluster expansion reaction exist). In a synthesis with a given metal, the product observed depends on the relative barrier heights of the steps as well as the reaction conditions.

Cluster Reactivities. Although the structural properties of the new clusters produced in this work are interesting, all obey the electron-counting rules. More importantly, the work defines a set stoichiometric reactions interconnecting stable compounds of defined structures. At this elementary level, this work, along with one earlier study,[52] establishes for the first time important aspects of the reactvity of the three isomeric forms of a dimetallapentaborane.

Scheme 5

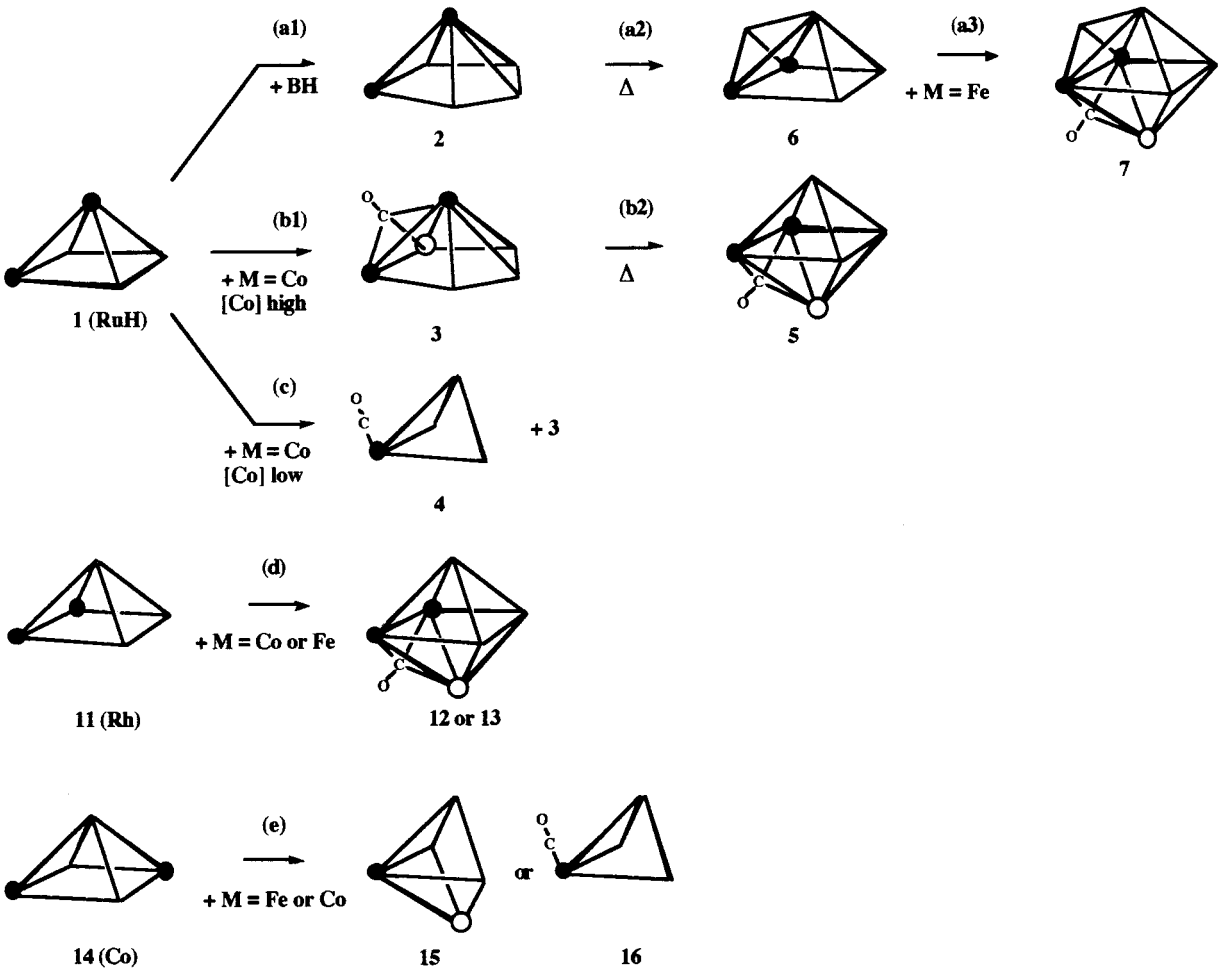

We chose to use BH_3·THF, $Fe_2(CO)_9$, and $Co_2(CO)_8$ as test reagents. Although each reagent has unique features, all are commonly used in cage- and cluster-building reactions.[7,77] In addition, thermolysis at modest temperatures (80−100 °C) was investigated. In the following, only reactions which give a single metallaborane product in good yield are considered significant for the purpose of this discussion. The observations are summarized in Scheme 5, where positive reactions are indicated by the reagents listed on the reaction arrow. Included in Scheme 5 are the previously published results on the reactions of *nido*-2,4-$(Cp^*Co)_2B_3H_7$, **14**, with $Fe_2(CO)_9$ to give *nido*-1-(Cp^*Co)-2-$\{Fe(CO)_3\}B_3H_7$, **15**, and with $Co_2(CO)_8$ to give *arachno*-$(Cp^*Co)(CO)B_3H_7$, **16** (Scheme 5d).[52]

Ruthenaborane **1** displays the most varied chemistry. It undergoes facile cluster expansion reactions with borane (Scheme 5a1) and with $Co_2(CO)_8$ (Scheme 5b1) to yield analogous nido six-atom clusters. Both compounds lose hydrogen on heating, with the former yielding a capped square pyramidal cluster (**6**, Scheme 5a2) and the latter a closo cluster (**5**, Scheme 5b2). As the sep of both clusters is the same, the difference in final structure is attributed to the differing numbers of endo hydrogens in the two compounds.[73] The open square face left because the capping option is adopted by **6** permits the addition of an iron fragment to give **7** (Scheme 5a3).

The observation of two distinct steps to reach the condensed clusters **5** and **6** demonstrates kinetic control of the fragment addition reactions. A more forceful demonstration of kinetic control comes from an examination of the reaction of **1** with differing amounts and concentrations of the reagent $Co_2(CO)_8$. Low levels of $Co_2(CO)_8$ give the cluster degradation product analogous to **16** (Scheme 5e) whereas high levels give metal fragment addition to give **3**. As $Co_2(CO)_8$ is well-known to generate $Co(CO)_4$ radicals[78] which participate in cluster reactions,[79] a simple explanation of the observations can be offered. Addition of a $Co(CO)_4$ radical to **1** would give a $\{(Cp^*Ru)_2(\mu\text{-}H)_2B_3H_7Co(CO)_4\}$ radical cluster intermediate. In the presence of relatively high concentrations of $Co(CO)_4$ radicals, bimolecular H atom abstraction to give $HCo(CO)_4$ and molecular-$\{(Cp^*Ru)_2(\mu\text{-}H)_2B_3H_6Co(CO)_4\}$ dominates and loss of H_2 generates **3** as the major product. With low concentrations of $Co(CO)_4$ radicals, unimolecular decomposition of the radical intermediate to **4** plus coproducts $[Cp^*Ru(CO)_2]_2$, $[Co(CO)_3]_4$, and H_2 (first two coproducts were spectroscopically observed) becomes competitive with the bimolecular process that forms **3**.

In contrast to **1**, **11** undergoes the addition of either Co or Fe fragments to give the closo cluster **12** or **13** in one step (Scheme 5d). It is tempting to suggest that a nido intermediate analogous to **3** is involved, but this would imply that the barrier to hydrogen elimination is considerably reduced in the change from RuH to Rh. More appealing is the addition of the metal fragment to give a distinct intermediate which reacts by two competitive

(77) *The Chemistry of Metal Cluster Complexes*; Shriver, D. F., Kaesz, H. D., Adams, R. D., Eds.; VCH: New York, 1990.

(78) Absi-Halabi, M.; Atwood, J. D.; Forbus, N. P.; Brown, T. L. *J. Am. Chem. Soc.* **1980**, *102*, 6248.

(79) Horwitz, C. P.; Holt, E. M.; Shriver, D. F. *Organometallics* **1985**, *4*, 1117.

pathways: insertion to give the nido cluster product vs elimination of hydrogen to give the closo product. If correct, the different reactivities of the three isomer types relative to the metal-based test reagents may be associated with the metal atom positions in the square pyramidal cluster. Conceptually, addition of the incoming metal fragment to an edge of the square face of **1**, **11**, or **14** leads to different metal arrangements. Why could this lead to different products?

In all cases when the metals are adjacent, the incoming metal fragment generates a metal triangle capped with a triply bridging CO ligand in the product (Scheme 5a3,b1,d). This structural feature is retained in the thermal conversion of **3** to **5** (Scheme 5b2), suggesting it provides some cluster stability. In the case of **1** and **14**, but not **11**, the generation of this feature would require cluster rearrangement. This additional contribution to the reaction barrier leading to a closo product permits other paths to compete effectively, e.g., Scheme 5b1. As suggested previously,[52] addition of the incoming metal moiety to a metal in the square face is a reasonable way to account for the fact that 1-(Cp*Co)-2-{$Fe(CO)_3$}B_3H_7, **15**, is observed rather than 1-{$Fe(CO)_3$}-2-(Cp*Co)B_3H_7 as the product of the reaction of **14** with $Fe_2(CO)_9$. These observations suggest a connection between the nature and position of the metal moieties in the dimetallaborane and the products observed.

Summary

A rational, useful synthetic route to *nido*-M_2B_3 clusters of Ru and Rh has been developed based on the reactions of monoboranes with monocyclopentadienylmetal chlorides. Relative to Cp*Rh in a dimetallaborane cluster, the Cp*Ru fragment compensates by incorporating an additional endo hydrogen into the cluster structure. In terms of geometry and hydrogen atom placement, the appropriate comparison is Cp*Rh with Cp*RuH. Directly or indirectly, the added endo hydrogen leads to a richer reaction chemistry for Ru vs Rh based on reactions with selected main group and transition metal fragments. The reactions observed suggest that fragment addition and hydrogen loss determine the product found. Metal positions in the *nido*-M_2B_3 cluster appear to be important in determining the cluster products observed under the mild conditions used. The reactions observed are consistent with known metal cluster chemistry,[4,77] but the fact that rather subtle factors such as cluster geometry, metal position, number of endo hydrogens, or reagent concentrations can determine product type for a dimetallaborane shows that only the barest outline of the reaction chemistry of multimetal metallaborares has been revealed thus far.

Note Added in Proof: After revision of this manuscript we learned that compounds **1** and **2** have been synthesized and characterized by others using a similar approach.[80]

Acknowledgment. Generous support of the National Science Foundation is gratefully acknowledged. We thank Mr. D. Schifferl for aid with the NMR experiments.

Supporting Information Available: X-ray crystallographic files, in CIF format, and tables giving information on data collection and reduction and structure solution and refinement, crystallographic parameters, atomic coordinates and equivalent isotropic temperature factors, bond distances, bond angles, and anisotropic temperature factors for **1**−**3**, **6**, **7**, **9**. This material is available free of charge via the Internet at http://pubs.acs.org. The crystal data and related metrics for **11** and **12** have been deposited elsewhere.[36]

JA982954J

(80) Kawano, Y.; Shimoi, M., personal communication.